International Journal of
Applied Sciences and Smart Technologies

Volume 02, Issue 01, June 2020

Solving Inverse Problems Interestingly
Rommel R. Real

Pricing the Financial Heston Model Using Parallel Finite Difference Method on GPU CUDA
Pranowo

Characteristics of Solar Still with Heat Exchangers on the Cover Glass
Ignasius Dinang Yudra Nanda, F. A. Rusdi Sambada, Yulianto, Angelina Boru Sitio

A Study of Statics on Driyarkara Electric Automobile Chassis Prototype
A. H. Astyanto, Y. R. Yanto, A. B. W. Adi

Area Under the Curves, Volume of Rotated, and Surface Area Rotated About Slanted Line
Billy Suandito

Comparison Simulation Analysis of the Gradual Summation of a Function with Recognition of Direct Extrapolation Via IN Series
Stephanus Ivan Goenawan

Application of Klein-4 Group on Domino Card
Asido Saragih, Santri Chintia Purba

Smart Campus Mobile Application Toward the Development of Smart Cities
Tanweer Alam, Yazeed Mohammed Alharbi, Firas Adel Abusallama, Ahmad Osama Hakeem

p-ISSN 2655-8564 & e-ISSN 2685-9432

International Journal of Applied Sciences and Smart Technologies

Volume 2, Issue 1, page i

p-ISSN 2655-8564, e-ISSN 2685-9432

CONTENTS

CONTENTS i

EDITORIAL BOARD ii

PREFACE iii

Solving Inverse Problems Interestingly 1–8
Rommel R. Real

Pricing the Financial Heston Model Using Parallel Finite Difference Method on GPU CUDA 9–22
Pranowo

Characteristics of Solar Still with Heat Exchangers on the Cover Glass 23–34
Ignasius Dinang Yudra Nanda, F. A. Rusdi Sambada, Yulianto, Angelina Boru Sitio

A Study of Statics on Driyarkara Electric Automobile Chassis Prototype 35–44
A. H. Astyanto, Y. R. Yanto, A. B. W. Adi

Area Under the Curves, Volume of Rotated, and Surface Area Rotated About Slanted Line 45–58
Billy Suandito

Comparison Simulation Analysis of the Gradual Summation of a Function with Recognition of Direct Extrapolation via IN Series 59–66
Stephanus Ivan Goenawan

Application of Klein-4 Group on Domino Card 67–74
Asido Saragih, Santri Chintia Purba

Smart Campus Mobile Application Toward the Development of Smart Cities 75–88
Tanweer Alam, Yazeed Mohammed Alharbi, Firas Adel Abusallama, Ahmad Osama Hakeem

AUTHOR GUIDELINES 89

International Journal of Applied Sciences and Smart Technologies

Volume 2, Issue 1, page ii

p-ISSN 2655-8564, e-ISSN 2685-9432

EDITORIAL BOARD

Editor in Chief
Dr. I Made Wicaksana Ekaputra *(Sanata Dharma University, Yogyakarta, Indonesia)*
Email: made@usd.ac.id

Associate Editor
Dr. Pham Nhu Viet Ha *(Vietnam Atomic Energy Institute, Hanoi, Vietnam)*
Dr. Hendra Gunawan Harno *(Gyeongsang National University, Jinju, The Republic of Korea)*
Dr. Iswanjono *(Sanata Dharma University, Yogyakarta, Indonesia)*
Dr. Mukesh Jewariya *(National Physical Laboratory, New Delhi, India)*
Dr. Mongkolsery Lin *(Institute of Technology of Cambodia, Phnom Penh, Cambodia)*
Dr. Yohanes Baptista Lukiyanto *(Sanata Dharma University, Yogyakarta, Indonesia)*
Dr. Apichate Maneewong *(Thailand Institute of Nuclear Technology, Bangkok, Thailand)*
Dr. Sudi Mungkasi *(Sanata Dharma University, Yogyakarta, Indonesia)*
Dr. Pranowo *(Universitas Atma Jaya Yogyakarta, Yogyakarta, Indonesia)*
Dr. Mahardhika Pratama *(Nanyang Technological University, Singapore)*
Dr. Augustinus Bayu Primawan *(Sanata Dharma University, Yogyakarta, Indonesia)*
Prof. Dr. Leo Hari Wiryanto *(Bandung Institute of Technology, Bandung, Indonesia)*

Editorial Proofreader
Ir. Ignatius Aris Dwiatmoko, M.Sc. *(Sanata Dharma University, Yogyakarta, Indonesia)*
P. H. Prima Rosa, S.Si., M.Sc. *(Sanata Dharma University, Yogyakarta, Indonesia)*

Editorial Assistant
Eduardus Hardika Sandy Atmaja, M.Cs. *(Sanata Dharma University, Yogyakarta, Indonesia)*
Vittalis Ayu, M.Cs. *(Sanata Dharma University, Yogyakarta, Indonesia)*

Administration
Catharina Maria Sri Wijayanti, S.Pd. *(Sanata Dharma University, Yogyakarta, Indonesia)*

Contact us
International Journal of Applied Sciences and Smart Technologies
Faculty of Science and Technology
Sanata Dharma University
Kampus III Paingan, Maguwoharjo, Depok, Sleman
Yogyakarta, 55282
Phone : +62 274883037 ext. 523110, 52320
Fax : +62 272886529
Email : editorial.ijasst@usd.ac.id
Website : http://e-journal.usd.ac.id/index.php/IJASST

IJASST is an open-access peer-reviewed journal that mediates the dissemination of research and studies conducted by academicians, researchers, and practitioners in science, engineering, and technology.

International Journal of Applied Sciences and Smart Technologies
Volume 2, Issue 1, page iii
p-ISSN 2655-8564, e-ISSN 2685-9432

PREFACE

We are honored to announce the publication of the International Journal of Applied Sciences and Smart Technologies (IJASST) for volume two issue one, which is the edition of June 2020. IJASST is an open access peer-reviewed journal that mediates the dissemination of survey and research results of academicians, researchers, and practitioners in engineering, science, technology, and basic sciences which relate to technology including applied mathematics, physics, and chemistry. IJASST accepts submission from all over the world.

This edition includes eight manuscripts from different institutions and subjects related to applied sciences and smart technologies. We always keep the quality of every published volume and issue by selecting the received manuscripts. All manuscripts follow the peer-reviewed procedure and processed using the open journal system (OJS) of IJASST. We believe that all the papers published in this issue will have a significant influence on this journal's scope.

We are convinced that IJASST will provide the opportunity to gain and present authentic and insightful scientific and technological information on the latest advances in science and technology. We are looking forward to your submission to IJASST for the next edition.

Dr. I Made Wicaksana Ekaputra
Editor in Chief
IJASST

This page intentionally left blank

International Journal of Applied Sciences and Smart Technologies

Volume 2, Issue 1, pages 1–8

p-ISSN 2655-8564, e-ISSN 2685-9432

Solving Inverse Problems Interestingly

Rommel R. Real[1,2]

[1]Mathematical Sciences Institute, College of Science, The Australian National University, Canberra, Australia
[2]Department of Mathematics, Physics, and Computer Science, University of the Philippines Mindanao, Mintal, Davao City, the Philippines
Corresponding Author: rommel.real@anu.edu.au

(Received 28-06-2019; Revised 17-10-2019; Accepted 17-10-2019)

Abstract

Inverse problems deal with recovering the causes for a desired or given effect. Their presence across sciences and their theoretical study can be traced to a classic example. Moreover, their ill-posedness motivates computational methods to solve them, and we give a very humble introduction to them. In relation we discuss their active research trends.

Keywords: divergence measure, ill-posed equation, inverse problem, regularization, noisy data

1 Introduction

Inverse problems are everywhere. The simplest example out there would be human vision. From measurements of scattered light that reaches our retinas, our brain constructs a detailed 3-dimensional image of the world around us. But how is this possible with only a limited number of points in our surroundings? Our brain has a way to complete the image by interpolating and extrapolating the data acquired from the identified points. Constructing this image is actually an example of what is called an inverse problem.

Volume 2, Issue 1, pages 1–8

p-ISSN 2655-8564, e-ISSN 2685-9432

There is no universal definition to inverse problems. One might say that inverse problems are concerned with determining causes for a desired effect [4]. The American mathematician J.B. Keller gave this well-cited definition [12]:

> "*We call two problems inverses of one another if the formulation of each involves all or part of the solution of the other. Often, for historical reasons, one of the two problems has been studied extensively for some time, while the other is newer and not so well understood*".

This implies that for an inverse problem to be defined, first there must be an underlying direct problem. We will consider some examples.

2 An Important Example

One of the most well-studied inverse problems is known as Calderón's problem. Back in 1980 A. P. Calderón published a paper "On an inverse boundary value problem". It aims to solve this problem: is it possible to determine the electrical conductivity of a medium by making voltage and current measurements at the boundary of the medium. This inverse method is also known as electrical impedance tomography (EIT). Interestingly, Calderón had been researching on this problem while working as a petroleum engineer for Argentina's state oil company back in 1947. He stayed there for a few years before embarking a full-time career in mathematics.

His paper became a ground-breaking one: it started a new era of mathematical research on inverse problem. Later on EIT would find itself applied in medical imaging. In fact, a prize for outstanding contribution in the field of inverse problems is named after him (check out Calderon Prize). You may check out Gunther Uhlmann's paper [16] for a summary of progress in Calderón's problem.

Calderón's problem is a good example on how real-world problems motivate mathematical research. In geophysics, one needs to explore the Earth's subsurface using reflected seismic waves. In ecology, space monitoring is used to assess trends of biological diversity using reconstructed satellite images. In medical imaging, tumors in a part of human body must be accurately detected from the attenuation of x-rays. Mathematically, these inverse problems are described using operator equations whose

Volume 2, Issue 1, pages 1–8
p-ISSN 2655-8564, e-ISSN 2685-9432

specific properties need to be studied with rigour. In fact, the progress in mathematical theory of inverse problems is independent of the growing applications, though the gap between them remains wide. This gap can be filled by showing more applications where the theoretical results hold, promoting a deeper appreciation of inverse problems.

3 Regularization

An inverse problem can be expressed as an operator equation in the form

$$F(x) = y, \tag{1}$$

for a specific exact data $y \in Y$, $F : X \to Y$ be a parameter-to-observation mapping between X, Y (they can be Hilbert, Banach, or even a general topological spaces), for a given parameter variable x. Inverse problems have one common property that makes them really hard to solve: they are *ill-posed*. In mathematics, a problem is well-posed if the following three are satisfied: the problem has a solution, it has a unique solution, and the solution depends continuously on the data. If one of the three is violated, the problem becomes ill-posed. For instance, the mathematical problem of EIT consists of a highly nonlinear partial differential equation, which is very ill-posed.

To address instability, we can solve the original ill-posed problem by solving a sequence of approximating well-posed problems. This technique is called regularization. Applying some numerical scheme (e.g. the ones from optimisation) to an ill-posed problem may lead to different solutions. Regularisation ensures a specific solution with desirable properties is recovered. For instance, suppose we have a noisy data $y^\delta \in Y$. Instead of solving the ill-posed equation (1), we solve an equivalent minimisation problem.

$$\min_{x \epsilon C} S(F(x), y^\delta) \tag{2}$$

for a an admissible set $C \subseteq X$ and $S : Y \times Y \to \mathbb{R}^+ \cup \{0\}$ be the divergence measure between the reconstrution $F(x)$ and the noisy data y^δ. Since (1) is ill-posed, (2) is also ill-posed, but easier to handle. Now we describe a very common regularization method. In variational regularization, we solve a surrogate of (2), given by

Volume 2, Issue 1, pages 1–8

p-ISSN 2655-8564, e-ISSN 2685-9432

$$\min_{x \in C} S\big(F(x), y^{\delta}\big) + \alpha R(x) \tag{3}$$

where $R : X \to \mathbb{R}^{+} \cup \{0\}$ is the penalty functional and $\alpha \in \mathbb{R}$ is a positive constant regularization parameter. Now, (3) is stable due to the promotion of the penalty term, and can be solved using optimisation algorithms. An example of (3) common in statistics and machine learning is Tikhonov regularization, or ridge regression, where normally the penalty term favors solutions with smaller norms, while the functional S is the least-squares functional. The parameter α serves as a trade-off between data fidelity and stability, and must be fine-tuned. If the regularization parameter α_* is chosen via a given *parameter choice rule* to solve (3), we can obtain the solution with this best possible trade-off. Moreover, finding an appropriate regularization parameter α_* to solve (3) is a very active of research in inverse problems, and usually done by imposing assumptions on the ill-posed problem.

Alternatively, iterative regularization can be used. To describe, let us assume X and Y to be Hilbert spaces with norm given by $\|.\|$. The simplest of this type is Landweber method, which is simply the gradient method applied to solving

$$\min_{x \in X} \|F(x) - y^{\delta}\|$$

Starting an initial guess $x_0 \in X$, the (nonlinear) Landweber iteration [5] is given by

$$x_{k+1}^{\delta} = x_k^{\delta} - \omega_k^{\delta} F'\big(x_k^{\delta}\big)^{*} \big(F\big(x_k^{\delta}\big) - y^{\delta}\big), \quad k = 0,1, \ldots \tag{4}$$

where ω_k^{δ} is a relaxation constant chosen often between 0 and 1 (can be constant for all k). Since the original problem (1) is ill-posed, (4) must be terminated after a finite number of iterations k_* to ensure the best reconstruction possible. In this case the iteration k_* acts as the regularization parameter. As in variational regularization, choosing an appropriate k_* using an appropriate parameter choice rule is also an active research area.

In some problems, variational regularization in terms of (3) may lead to solving large and sparse systems of equations, which can be computationally expensive. In addition, for every value of α taken from an interval (e.g. exponential grid), a full numerical scheme must be implemented to solve to solve. In contrast, iterative regularization have lesser computational burden, but could take a large number of iterations. Due to this

Volume 2, Issue 1, pages 1–8
p-ISSN 2655-8564, e-ISSN 2685-9432

observation, iterative methods are known to be slow but reliable, which makes them more preferred.

However, variational regularization has one important advantage: it can be formulated for problems using generalized divergence/residual terms $S(F(x), y^{\delta})$ where S in (3) does not have to be a norm in Banach spaces. Some instances are in EIT, where the measurement error of the data could depends on the location of the measurement (i.e. error is larger in areas closer to the ultrasound receiver). This is also the case when measuring probability measures. For a convenient overview of these methods, the reader may refer to [9,13].

Lately, in some publications theoretical results often in this research area go hand-in-hand with numerical examples. Some numerical examples come from anywhere optimal control, plasma physics, economics, etc. Theoretical results usually involve convergence rates, in terms of the noise level $\delta := S(y, y^{\delta})$, they allow comparisons between regularization methods. However this is not be doable in some settings, such as for iterative regularization methods in Banach spaces [8,11,14]. The more important type of theoretical result is the proof of regularization property: given a parameter choice rule, the approximate solution produced by the regularization method should converge to the (unknown) desired exact solution as the noise level decays.

4 Current Trends

Now i want to cite some important research trends in the field of regularization for inverse problems. One of the most well-studied types of parameter choice rules is the discrepancy principle, which states to pick the regularization parameter k_* or α_* once the residual becomes smaller than a multiple of the noise level. Mathematically, for iterative methods it means to pick k_* such that

$$S(F(x_{k_*}^{\delta}), y^{\delta}) \leq \tau\delta < S(F(x_k^{\delta}), y^{\delta}), \quad 0 \leq k \leq k_*$$

for a given $\tau > 1$. For both variational and iterative regularization methods this has been well-studied [4,5,14]. However, notice that aside from the noisy data y^{δ}, the discrepancy principle requires information of the noise level δ. In some instances such

Volume 2, Issue 1, pages 1–8
p-ISSN 2655-8564, e-ISSN 2685-9432

information may not available, and either overestimation or underestimation of the noise level may lead to an unsatisfactory solution of the inverse problem. Hence, for regularization methods, it is necessary to develop heuristic rules which do not need the noise level. Although Bakushinskii's veto [1] states that heuristic rules cannot lead to convergence in the worst case scenario for any regularization method, it is still possible to prove some convergence results under such rules under specific assumptions on the noisy data. A well-studied heuristic rule was formulated by Hanke and Raus [6] and it has been developed since then, for instance in [7].

Another growing trend is studying regularization methods in Banach spaces. The standard reference book [4] compiles fundamental results under Hilbert spaces. The need for extending these results towards Banach spaces stems out naturally when the sought solution is non-smooth, e.g. when it is sparse or piecewise constant. Hilbert spaces are too smooth to cover such solutions. A strategy is to introduce a nonsmooth penalty term, which includes the l_1-norm and the total variation (TV), in iterative regularization [2,8]. For variational regularization, one way to obtain convergence results is to impose more general conditions on the sought solution [7]. Obtaining results under Banach spaces also allows to cover both linear and nonlinear problems, leading to more computationally challenging examples [15]. This is a great development since many inverse problems are expressed in terms of highly nonlinear partial differential equations, leading to nonlinear and often non-differentiable forward operators. In this area obtaining convergence results using more general assumptions and extending them towards general topological spaces [13] is still very active.

Another important issue involves the forward operator. For instance, problem (4) is formulated assuming F is differentiable, in a more general sense. It is possible to obtain a modified Landweber method where instead of the derivative of F, an operator approximating the derivative can be used, leading to a derivative-free iterative method [10], Chapter [4]. So far only a few types of derivative-approximating operators have been known [3], and different types may lead to different convergence analyses. Exploring more problems with nonsmooth forward operators is always a welcome research area. In some problems where the direct problem involves not fully linear

PDEs, the corresponding forward operator may be too complicated to formulate, so solving inverse problems with it would be necessary.

5 Conclusion

Inverse problems are still starting to gain better understanding, dating back around thirty years. It's an area that requires expertise in computational maths, such as in solving PDEs to optimisation. Obtaining theoretical result involves lots of estimation in various settings, from Banach spaces to Sobolev spaces! It's a relatively new area that needs more people to move in!

References

[1] A. B. Bakushinskii, "Remarks on choosing a regularization parameter using the quasioptimality and ratio criterion," *USSR Computational Mathematics and Mathematical Physics,* **24** (4), 181−182, 1984.

[2] R. Bot and T. Hein, "Iterative regularization with a general penalty term-theory and applications to L^1 and tv regularization," *Inverse Problems,* **28** (10), Article ID 104010, 1−19, 2012.

[3] C. Clason and V. H. Nhu, "Bouligand-Landweber iteration for a non-smooth ill-posed problem," *Numerische Mathematik,* **142** (4), 789−832.

[4] H. W. Engl, M. Hanke, and A. Neubauer, *Regularization of Inverse Problems,* Kluwer Academic Publishers, London, 1996.

[5] M. Hanke, A. Neubauer, and O. Scherzer, "A convergence analysis of the landweber iteration for nonlinear ill-posed problems," *Numerische Mathematic,* **72** (1), 21−37, 1995.

[6] M. Hanke and T. Raus, "A general heuristic for choosing the regularization parameter in ill-posed problems," *Society for Industrial and Applied Mathematics Journal on Scientific Computing,* **17** (4), 956−972, 1996.

[7] Q. Jin, "Hanke-Raus heuristic rule for variational regularization in banach spaces," *Inverse Problems,* **32** (8), Article ID 085008, 1−18, 2016.

Volume 2, Issue 1, pages 1–8

p-ISSN 2655-8564, e-ISSN 2685-9432

[8] Q. Jin, "Landweber-Kaczmarz method in banach spaces with inexact inner solvers," *Inverse Problems,* **32** (10), Article ID 104005, 1−26, 2016.

[9] B. Kaltenbacher and A. Klassen, "On convergence and convergence rates for ivanov and morozov regularization and application to some parameter identification problems in elliptic PDEs," *Inverse Problems,* **34** (5), article ID 055088, 1−24, 2018.

[10] B. Kaltenbacher, A. Neubauer, and O. Scherzer, *Iterative Regularization Methods for Nonlinear Ill-Posed Problems,* Walter de Gruyter GmbH & Co. KG, Berlin, 2008.

[11] B. Kaltenbacher, F. Schöfer, and T. Schuster, "Iterative methods for nonlinear ill-posed problems in banach spaces: convergence and applications to parameter identification problems," *Inverse Problems*, **25** (6), article ID 065003, 1−19, 2009.

[12] J. B. Keller, "Inverse problems," *The American Mathematical Monthly,* **83** (2), 107−118, 1976.

[13] C. Poschl, *Tikhonov Regularization with General Residual Term*, Dissertation, Leopold Franzens Universität Innsbruck, 2008.

[14] F. Schöpfer, A. K. Louis, and T. Schuster, "Nonlinear iterative methods for linear ill-posed problems in banach spaces," *Inverse Problems*, **22** (1), 311−329, 2006.

[15] T. Schuster, B. Kaltenbacher, B. Hofmann, and K. S. Kazimierski, *Regularization methods in Banach Spaces,* Walter de Gruyter GmbH & Co. KG, Berlin, 2012.

[16] G. Uhlmann, "30 Years of Calderón's Problem", *Séminaire Laurent Schwartz-EDP et applications*, École Polytechnique, 1−25, 2012-2013.

International Journal of Applied Sciences and Smart Technologies

Volume 2, Issue 1, pages 9–22

p-ISSN 2655-8564, e-ISSN 2685-9432

Pricing the Financial Heston Model Using Parallel Finite Difference Method on GPU CUDA

Pranowo

Department of Informatics Engineering, Faculty of Industrial Technology, Universitas Atma Jaya Yogyakarta, Indonesia
Corresponding Author: pranowo@uajy.ac.id

(Received 29-04-2019; Revised 17-10-2019; Accepted 17-10-2019)

Abstract

An option is a financial instrument in which two parties agree to exchange assets at a price or strike and the date or maturity is predetermined. Options can provide investors with information to set strategies so they can increase profits and reduce risk. Option prices need to be accurately evaluated according to reality and quickly so that the resulting value can be utilized at the best momentum. Valuation of option prices can use the Heston equation model which has advantages compared to other equation models because the assumption of volatility is not constant with time or stochastic volatility. The volatility that is not constant with time corresponds to reality because the underlying asset as a basis can experience fluctuations. The Heston equation has a disadvantage because it is a derivative equation that is difficult to solve. One way to solve derivative equations easily is to use a numerical solution to the finite difference method of non-uniform grids because the Heston equation can be assumed to be a parabolic equation. The numerical solution of the finite difference method can solve derivative equations flexibly and do not require matrix processing. But it requires a heavy and slow computing process because there are many elements of

Volume 2, Issue 1, pages 9–22
p-ISSN 2655-8564, e-ISSN 2685-9432

calculation and iteration. This study proposes a numerical solution to the finite difference method by using the Compute Unified Device Architecture (CUDA) parallel programming to solve the Heston equation model that applies the concept of stochastic volatility to get accurate and fast results. The results of this research proved 15.52 times faster in conducting parallel computing processes with error of 0.0016..

Keywords: option price, heston model, finite difference, parallel, GPU CUDA.

1 Introduction

Options provide investors with information to set strategies so they can increase profits and reduce risk. Valuation of option prices can be assessed using the Heston equation model that applies stochastic volatility, which means that something is determined randomly and may not be accurately predicted.

Research related to numerical solution of option price using Heston model been done previously which can be seen in Table 1. Researchers indicate that previous research was limited to solving Heston equations using numerical solutions for option prices and had not been implemented in parallel computing so that this study discussed the numerical solutions of finite methods difference non-uniform grids to solve Heston equations in parallel computing.

The computational process of the finite difference method of non-uniform grids will increase as the number of grids increases. Heavy computing process is an obstacle in using many grids to improve the accuracy of results. At first, the computer had only one Central Processing Unit (CPU) or called the uniprocessor architecture for computational processing. Today computers evolve into multicore architectures that support processing in parallel. Parallel processing can be done with parallel programming, namely programming that focuses on solving problems simultaneously using fully using the computational power of computer architecture [1]. These problems can be solved by computational processing using parallel programming that utilizes the Graphics Processor Unit (GPU) with the Compute Unified Device Architecture (CUDA)

Volume 2, Issue 1, pages 9–22

p-ISSN 2655-8564, e-ISSN 2685-9432

Programming Model. GPU consists of a set of CPU's that perform computational processes in parallel so that it can work on many computational processes simultaneously. CUDA Programming Model is an application programming model that utilizes GPU as the core computational process. The solution to the numerical problem of derivative equations in the Heston model using the finite difference method that utilizes CUDA Programming Model-based parallel programming is expected to determine accurate option values with fast computational performance.

Table 1. Previous research

Research	Purpose
Diamond–Cell Finite Volume Scheme for the Heston Model [7]	Propose a new numerical scheme to solve partial equations that appear in the Heston stochastic volatility model.
Stability of central finite difference schemes for the Heston PDE [8]	Measuring stability limits is useful for time discretization methods in numerical solutions of Heston partial differential equations that stand out from mathematical finance.
Pricing European Options with Proportional Transaction Costs and Stochastic Volatility Using a Penalty Approach and a Finite Volume Scheme [9]	Establishing European standard option pricing values based on proportional and stochastic volatility transaction cost using the penalty approach method and finite volume scheme.
Numerical methods to solve PDE models for pricing business companies in different regimes and implementation in GPUs [10]	Solving the problem of corporate valuation models using a numerical approach to the finite difference method developed with parallelization using GPU technology.
Pricing of early-exercise Asian options under Lévy processes based on Fourier cosine expansions [11]	Set prices for Asian options with initial training features based on two-dimensional integration and backward recursion from Fourier coefficients in several numerical techniques implemented on the GPU.

2 Theory

2.1. Option Price

An option is a financial instrument in which two parties agree to exchange assets at a price or strike and the date or maturity is predetermined [2]. By paying in advance,

Volume 2, Issue 1, pages 9–22
p-ISSN 2655-8564, e-ISSN 2685-9432

known as price or premium from options, contract holders have the right, but not the obligation, to buy or sell assets at the time of maturity [3]. For example, the European option model has rules that can only be exercised at maturity.

The value of the option is based on the derivative value of the underlying asset, so the option is derivative. Based on this, the option contract is one of "derivative security" [4]. The underlying asset value has a property proportional to the value of the call option and the property is inversely proportional to the value of puts option. The value of up option calls if the value of the underlying asset rises and vice versa. The value puts down if the underlying asset rises and vice versa.

2.2. *Finite Difference for Heston PDE*

The finite difference method has the idea of discretizing domains with several grid points and using the finite difference to estimate derivatives at these grids [5]. The Finite Difference method assumes that the model grids can be structured or unstructured. The finite difference method is a technique to get numerical estimates from PDE.

To be able to implement finite difference to solve Heston PDE, it is necessary to discretize grids for the stock price and variance variables and discretize grids for maturity. This research uses non-uniform grids to discretize grids. Non-uniform grids have irregular grid distances between the two variables used. Non-uniform grids can be refined at certain points so that accurate price valuations can be produced with accurate prices using a few grid points.

The variables used to form grids are S, v, and t. It is necessary to determine the maximum value and the minimum value of S, v, and t as the value limit. The maximum value is denoted as S_{max}, v_{max}, and t_{max}. The values of S_{max} and $V_{max}$are obtained based on the calculated option case, while $t_{max} = \tau$ based on the maturity time. The minimum value is denoted as S_{min}, v_{min}, and t_{min}. The minimum value will always be set to $S_{min} = v_{min} = t_{min} = 0$ as the lower limit [6].

Volume 2, Issue 1, pages 9–22

p-ISSN 2655-8564, e-ISSN 2685-9432

The grid size is set with $N_s + 1$ point for the stock price, $N_v + 1$ point for volatility, and $N_T + 1$ point for maturity. The width of non-uniform grids for $N_s + 1$ stock price is arranged by equation

$$S_i = K + csinh(\xi_i), i = 0,1, \dots, N_s \quad (1)$$

The width of non-uniform grids for $N_v + 1$ volatility is arranged by equation

$$v_i = dsinh(j\Delta\eta), j = 0,1, \dots, N_V \quad (2)$$

The width of non-uniform grids for $N_t + 1$ volatility is arranged by equation

$$t_i = i \times dt, n = 0,1, \dots, N_T \quad (3)$$

This Heston PDE model estimates the point values in the interior and boundary sections separately. The interior part (S_i, v_i) is estimated by using first-order derivatives with a central difference. The boundary section is governed by certain conditions.

The boundary section has several conditions that need to be initialized, i.e. the conditions at maturity, S = S_{min} S = S_{max}, V = V_{max}, and V = V_{min}.

The boundary conditions at maturity, t = 0, the value of the call option is the intrinsic value (payoff) so that the equation is obtained.

$$U(S_i, v_j, 0) = max(0, S_i - K) \quad (4)$$

with a limit $i = 0, 1, \dots, N_s$ and $j = 0, 1, \dots, N_v$.

The boundary condition when S = S_{min} = 0, the call option becomes useless. Because that equation is obtained

$$U(0, v_j, t_n) = 0 \quad (5)$$

with a limit of $n = 0, 1, \dots, N_T$ and $j = 0, 1, \dots, N_v$.

The boundary condition when S = S_{max}, the equation used is

$$U(S_{max}, v_j, t_n) = S_{max} \quad (6)$$

with a limit of $n = 0, 1, \dots, N_T$ and $j = 0, 1, \dots, N_v$.

The boundary condition when V = V_{max}, the equation used is

$$U(S_i, v_{max}, t_n) = S \quad (7)$$

with a limit of $n = 0, 1, \dots, N_T$ and $i = 0, 1, \dots, N_s$.

Volume 2, Issue 1, pages 9–22

p-ISSN 2655-8564, e-ISSN 2685-9432

The boundary conditions when $V = V_{min} = 0$, the equation used is 2, namely $\frac{\partial U}{\partial S}$ which is solved using the central difference and $\frac{\partial U}{\partial v}$ which are resolved using forward difference. The equation formed is

$$\frac{\partial U}{\partial S}(S_i, 0, t_n) = \frac{U^n_{i+1,0} - U^n_{i-1,0}}{S_{i+1} - S_{i-1}}, \qquad \frac{\partial U}{\partial v}(S_i, 0, t_n) = \frac{U^n_{i,1} - U^n_{i,0}}{v_1} \tag{8}$$

Explicit schemes will be used as a technique to solve the finite difference. The equation used to obtain the elements $U^{n+1}_{i,\mathrm{j}}$ is

$$U^{n+1}_{i,j} = U^n_{i,j} + dt\left[\frac{1}{2}v_j S_i^2 \frac{\partial^2}{\partial S^2} + \frac{1}{2}\sigma^2 v_j \frac{\partial^2}{\partial V^2} + \rho\sigma v_j S_i \frac{\partial^2}{\partial v \partial S} + (r-q)S_i \frac{\partial}{\partial S} + \kappa(\theta - v_j)\frac{\partial}{\partial v} - r\right]U^n_{i,j} \tag{9}$$

2.3. Compute Unified Device Architecture (CUDA) Programming Structure

The CUDA programming model can execute applications on heterogeneous computing systems by only annotating code with a set of extensions to the C programming language. NVIDIA can be used to allocate the right host memory (CPU) and device (GPU) so that applications can be optimized and maximize the use of hardware [1]. The structure of the CUDA application process can be seen in Figure 1.

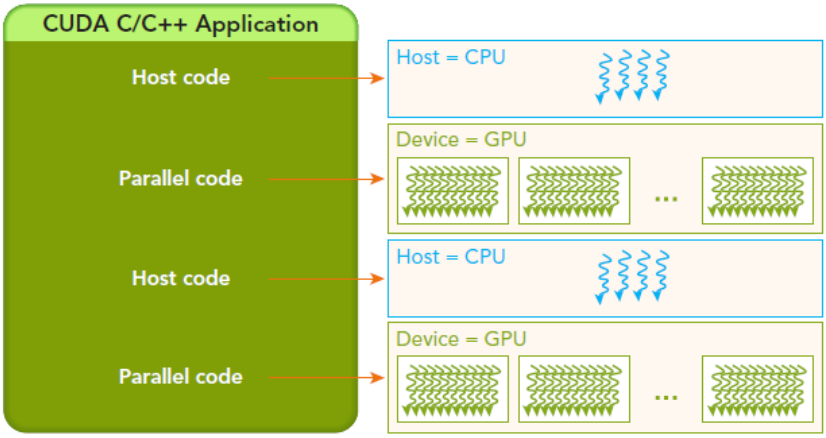


Figure 1. CUDA programming structure

CUDA which consists of serial code is run on the host, while parallel code is run on the GPU device. Host code is written in ANSI C and Device code is written using CUDA C. All code can be placed in a single source file or can use multiple source files

Volume 2, Issue 1, pages 9–22
p-ISSN 2655-8564, e-ISSN 2685-9432

to build the desired application or library. Codes that have been created for hosts and devices can be run using NVIDIA C Compiler (NVCC).

3 Algorithm

Parallel programming is a programming algorithm that forms a program that is capable of working on several processes in parallel utilizing multiple processors. In programming, CUDA uses SIMT (Single Instruction, Multiple Threads) execution models that are similar to SIMD (Single Instruction, Multiple Data) execution models for general data parallel programming [10]. The CUDA code execution unit, the kernel, executes simultaneously a set of threads in each block freely. Each thread will run one processor simultaneously on the same but different data instructions. Figure 2 describes the CPU and GPU algorithms.

Based on the flowchart above, it can be seen that the GPU algorithm can simplify the CPU algorithm so that it is not complex, where simple processes such as temporary grid updates, u, can be done simultaneously with boundary initialization. Therefore the GPU algorithm is simpler and not much repetitive. Repetition is only done to do time iterations. The 2-D matrix used is changed to $1-D$, because GPUs have different matrix index concepts. The CPU index is a row of x columns, $U\,[i \ldots Ns]\,[i \ldots Nv]$, and an index on the GPU in the form of columns x rows, $U\,[v \ldots Nv]\,[i \ldots Ns]$. GPU uses column x row index because it adjusts the hierarchy of blocks and threads. Changing the index to $1-D$ makes the matrix index can be adjusted according to the indexing formula $((ni * 1) + 1)$ in order to meet the concept of matrix CPU and GPU. In addition, memory allocation is only done in the matrix pointer U, u, S, V to allocate memory pointers on the device, GPU and copy values from the host, CPU to device, GPU. Another parameter that is not a pointer can be used directly across hosts and devices.

International Journal of Applied Sciences and Smart Technologies

Volume 2, Issue 1, pages 9–22

p-ISSN 2655-8564, e-ISSN 2685-9432

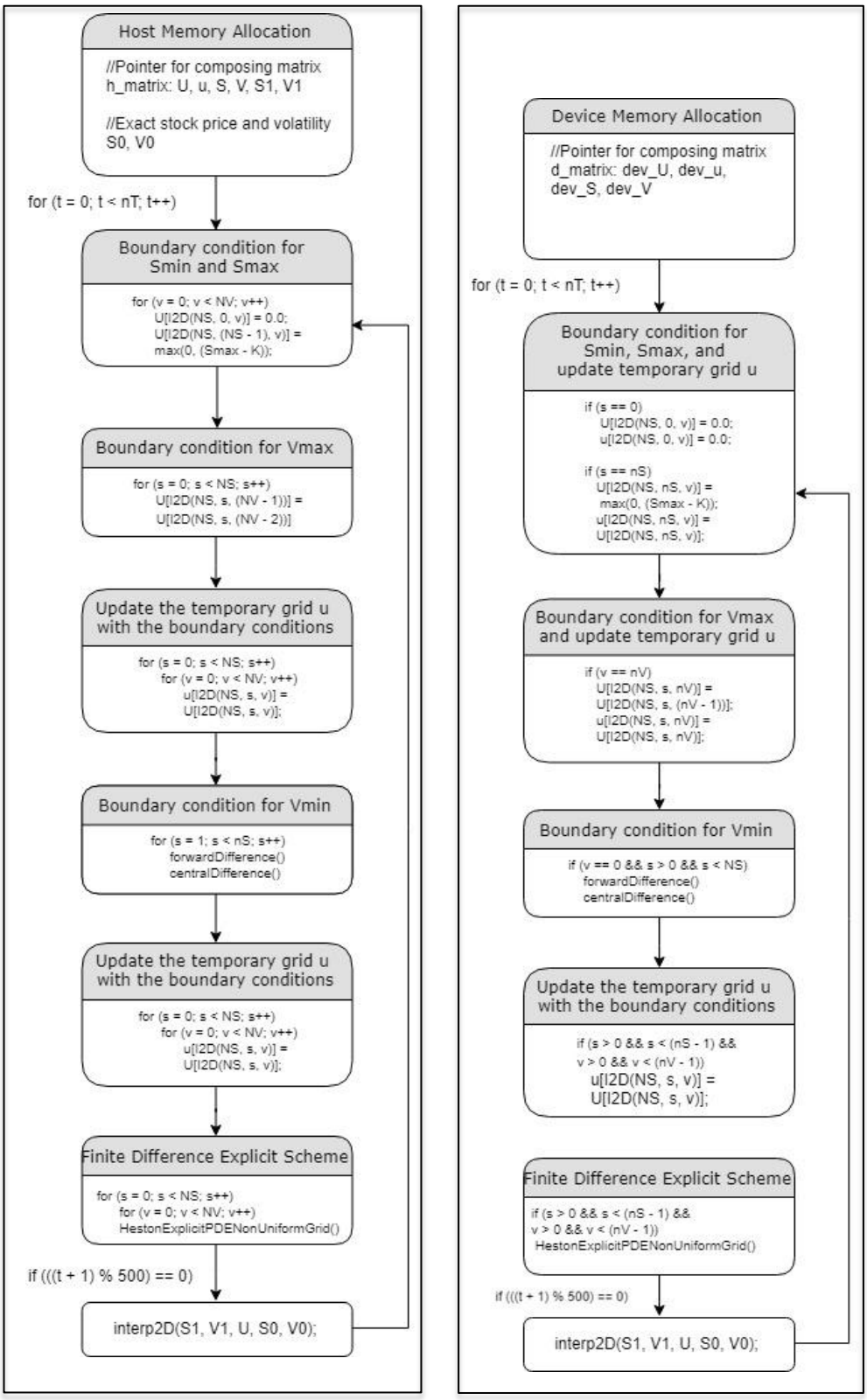


Figure 2. Flowchart of CPU (left) and GPU (right) algorithms

International Journal of Applied Sciences and Smart Technologies
Volume 2, Issue 1, pages 9–22
p-ISSN 2655-8564, e-ISSN 2685-9432

Finite difference non-uniform grids numerical solutions require complex and many computational processes, so that an increase in the number of relevant grids can be used to measure computational performance. This study conducted a numerical experiment by increasing the number of phased grids to see the difference between the performance of the GPU algorithm and the CPU algorithm. Experiments have been carried out on stand-alone computers with Intel Core i7 $8700K$ which has 6 cores with 3.7 GHz clock, 16 GB RAM, and Nvidia Geforce GTX 1080 Ti GPU which has 3584 processors and 11117 MB GDDR5X. The CUDA version installed is 9.0.

4 Results and Discussions

The implementation of the GPU algorithm to solve the equations of the Heston model using the finite difference method non-uniform grids needs to be verified. Verification is done by conducting numerical experiments to see the convergence of numerical finite difference non-uniform grids with exact values, along with the increase in the number of grid points for stock prices and volatility. The parameter used for this numerical experiment is $S_{max} = 200$; $V_{max} = 0.5$; $T_{max} = 0.15$; $K = 100$; $r = 0.02$; $q = 0.5$; $\sigma = 0.3$ and $\rho = -0.9$.

The combination of the number of grid points for the stock price and the volatility used varies. The size of the grids is formed by following the condition that finer grids approach the strike price K and around the point $v_0 = 0$. The number of grids for the stock price, N_s, has a range of values from 80 to 190, with 10 increases. The number of grids for the stock price, N_v, has a range of values from 20 to 75, with 5 increases. This numerical experiment will be an iterated as much as $N_t = 3000$ as the number of time points. The maximum grid combination in this experiment is $N_s = 190$ and $N_v = 75$. Non-uniforms grids can be seen in Figure 3**.**

International Journal of Applied Sciences and Smart Technologies

Volume 2, Issue 1, pages 9–22

p-ISSN 2655-8564, e-ISSN 2685-9432

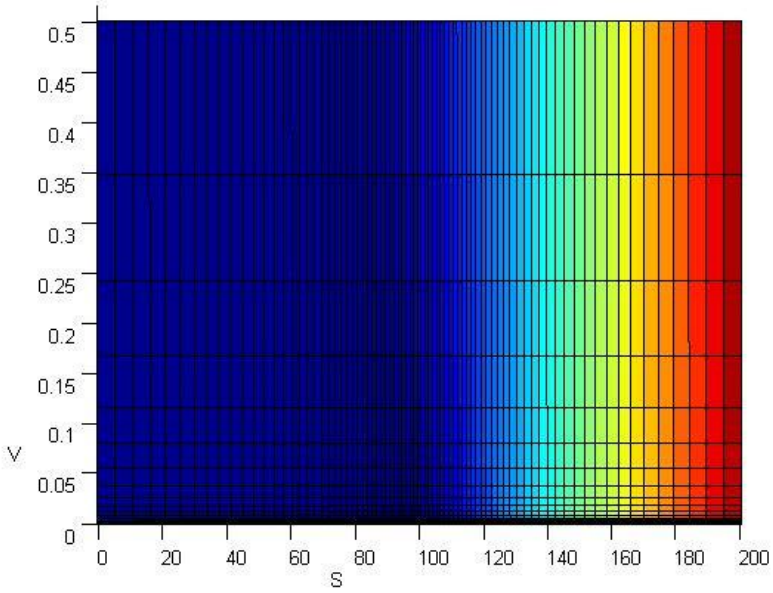


Figure 3. Non-uniform grids

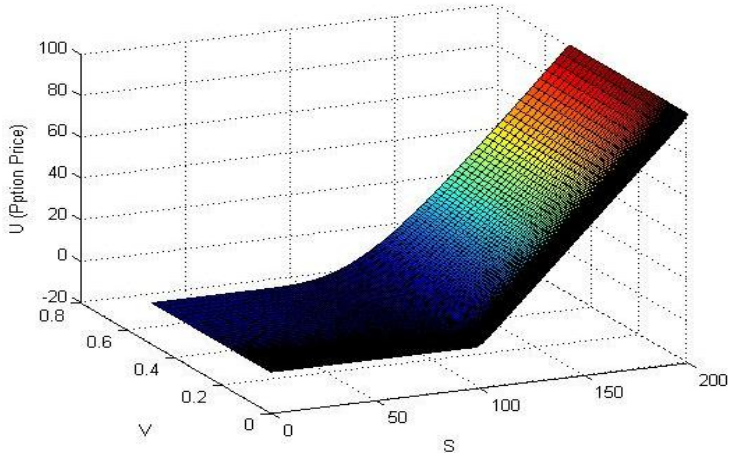


Figure 4. Surface prices use finite difference non-uniform grids $N_s = 190$ and $N_v = 75$

The exact value of the stock price, $S = 102$ and volatility, $v = 0.05$ with the exact value of the option price using the closed form solution of the Heston model is 4.2783. The results of finite difference non-uniform grids with a combination of up to grids $N_s = 190$ and $N_v = 75$ can be seen in Table 2 resulting in a value of 4.2801 using the GPU algorithm and 4.2805 using the CPU algorithm. Experiments were also carried out by increasing grid N_s and N_v to reach the limit before instability was achieved. The results obtained show grids $N_s = 190$ and $N_v = 150$ are the limits before instability is achieved.

International Journal of Applied Sciences and Smart Technologies

Volume 2, Issue 1, pages 9–22

p-ISSN 2655-8564, e-ISSN 2685-9432

Table 2. Relative error numerical finite difference non-uniform grids CPU and GPU solutions

N_s	N_v	CPU		GPU	
		Price	**Error**	**Price**	**Error**
80	20	4.2767	-0.0016	4.2760	-0.0023
90	25	4.2868	0.0085	4.2864	0.0081
100	30	4.2811	0.0028	4.2807	0.0024
110	35	4.2797	0.0014	4.2792	0.0009
120	40	4.2814	0.0031	4.2810	0.0027
130	45	4.2808	0.0025	4.2804	0.0021
140	50	4.2812	0.0029	4.2808	0.0025
150	55	4.2819	0.0036	4.2814	0.0031
160	60	4.2796	0.0013	4.2792	0.0009
170	65	4.2800	0.0017	4.2796	0.0013
180	70	4.2813	0.0030	4.2809	0.0026
190	75	4.2805	0.0022	4.2801	0.0018
190	150	4.2705	-0.0078	4.2799	0.0016

The error is obtained by calculating the difference in the option price of the numerical result with the exact value. The error in the experimental results has a variety of values, where at each increase in the number of grids, the error does not always decrease. If we look further, the overall error continues to decrease as grid size increases. In the maximum grid combination $N_s = 190$ and $N_v = 150$, the smallest is obtained obtained at 0.0016. So that it can be ascertained that increasing the number of grid points will increase accuracy. Table 3 shows the GPU algorithm can produce values that are closer to the exact values and are more accurate when grids are enlarged. Enlargement grids also run faster when processed using the GPU, compared to when processed using CPU results per exact price, CPU numeric, and numerical GPU. The price-end-result using non-uniform finite difference grids $N_s = 190$ and $N_v = 75$ after an iteration of $N_t = 3000$ is shown in Figure 4.

Comparison of GPU algorithm performance with CPU algorithm was done by conducting numerical experiments by increasing the number of phased grids can be seen in Table 3.

International Journal of Applied Sciences and Smart Technologies

Volume 2, Issue 1, pages 9–22

p-ISSN 2655-8564, e-ISSN 2685-9432

Tabel 3. Performance: CPU vs GPU with 3000 time steps (N_t) and various grids

N_s	N_v	Grid points	CPU Time (s)	GPU Time (s)	Speedup (times)	Speedup (s)
80	20	1600	0.243	0.176	1.38X	0.067
90	25	2250	0.348	0.171	2.04X	0.177
100	30	3000	0.467	0.172	2.72X	0.295
110	35	3850	0.607	0.171	3.55X	0.436
120	40	4800	0.766	0.179	4.28X	0.587
130	45	5850	0.921	0.179	5.15X	0.742
140	50	7000	1.111	0.181	6.14X	0.93
150	55	8250	1.321	0.176	7.51X	1.145
160	60	9600	1.547	0.181	8.55X	1.366
170	65	11050	1.793	0.186	9.64X	1.607
180	70	12600	2.033	0.182	11.17X	1.851
190	75	14250	2.323	0.193	12.04X	2.13
190	150	28500	4.765	0.307	15.52X	4.458

Based on the experimental results, stable GPU performance is always superior to the CPU. In finer grids as they approach the K strike price and around the point $v_0 = 0$, the grid sizes of N_s and N_v are increases $N_s + 10$ and $N_v + 5$ gradually, GPU performance continues to increase $12.04X$ faster. Experiments were also carried out by increasing N_v grids to reach the limit before instability was achieved. The results are obtained on the grids $N_s = 190$ and $N_v = 150$ where computing performance reaches $15.52X$ faster. The bigger the grid, the CPU performance will decrease while the GPU performance is stable.

5 Conclusions

This study aims to solve the equations of the Heston model using numerical solutions with finite difference non-uniform grids based on the Compute Unified Device Architecture (CUDA) parallel programming to get accurate and fast results. Based on this research, finite difference non-uniform grids with GPU algorithms can produce values that approach exact values and are more accurate when grids are enlarged.

The error in the experimental results continues to decrease every time N_s is increased by 10 points, and N_v is increased by 5 points. The results of the finite difference non-

uniform grids numerical solution with a maximum combination of grids $N_s = 190$ and $N_v = 75$ produce a value of 4.2805 with an error of 0.0018, compared to the combination value of internal grids $N_s = 80$ and $N_v = 20$ that produces a value of 4.2760 with an error of -0.0023. In the stability experiment with a combination of grids $N_s = 190$ and $N_v = 150$, the error obtained descreases to 0.0016. This proves that increasing the number of grid points will increase accuracy.

Enlargement grids also run faster when processed with the GPU. The computational process is faster 1.38 times in the combination of initial grids $N_s = 80$ and $N_v = 20$ and continues to increase until it has an acceleration of $12.04X$ faster on the grid $N_s = 190$ and $N_v = 75$. In the stability experiment with a combination of grids $N_s = 190$ and $N_v = 150$, computing performance reaches $15.52X$ faster.

Acknowledgements

This research was supported in part by Universitas Atma Jaya Yogyakarta (UAJY). This research was conducted using the GPU computers in the Graduate Program of Informatics Engineering UAJY.

References

[1] P. Kutik and K. Mikula, "Diamond–cell finite volume scheme for the heston model," *Discrete & Continuous Dynamical Systems*, **8** (5), 913−931, 2015.

[2] K. J. in't Hout and K. Volders, "Stability of central finite difference schemes for the heston PDE," *Numerical Algorithms*, **60** (1), 115−133, 2012.

[3] W. Li and S. Wang , "Pricing european options with proportional transaction costs", *Computers and Mathematics with Applications*,**73** (11), 2454−2469, 2017.

[4] D. Castillo, A. M. Ferreiro, J. A. García-Rodríguez, and C. Vázquez," Numerical methods to solve PDE models for pricing business companies in different regimes and implementation in GPUs," *Applied Mathematics and Computation*, **219** (24), 11233−11257, 2013.

Volume 2, Issue 1, pages 9–22

p-ISSN 2655-8564, e-ISSN 2685-9432

[5] B. Zhang and C. W. Oosterlee, "Pricing of early-exercise Asian options under Lévy processes based on Fourier cosine expansions," *Applied Numerical Mathematics*, **78**, 14−30, 2014.

[6] J. Cheng, M. Grossman, and T. McKercher, *Professional CUDA C Programming*, John Wiley & Sons, Indianapolis, 2014.

[7] E. Tandelilin, *Portofolio dan Investasi: Teori dan Aplikasi,* Kanisius, Yogyakarta, 2010.

[8] G. I. Ramírez-Espinoza, "Conservative and finite volume methods for the pricing problem," *Master Thesis*, Faculty of Mathematics and Natural Science, Bergische Universität Wuppertal, Wuppertal, 2011.

[9] T. F. Crack, *Basic Black-Scholes: Option Pricing and Trading*, 2009.

[10] Y. Chen, "Numerical Methods for Pricing Multi-Asset Options," *Master Thesis*, Graduate Department of Computer Science, University of Toronto, Toronto, 2017.

[11] F. D. Rouah, *The Heston Model and Its Extensions in Matlab and C#,* John Wiley & Sons, Hoboken, 2013.

International Journal of Applied Sciences and Smart Technologies

Volume 2, Issue 1, pages 23–34

p-ISSN 2655-8564, e-ISSN 2685-9432

Characteristics of Solar Still with Heat Exchangers on the Cover Glass

Ignasius Dinang Yudra Nanda[1,*], F. A. Rusdi Sambada[1], Yulianto[1], Angelina Boru Sitio[2]

[1]*Department of Mechanical Engineering, Sanata Dharma University, Yogyakarta, Indonesia*

[2]*Department of Mathematics and Natural Sciences Education, Sanata Dharma University, Yogyakarta, Indonesia*

[*]*Corresponding Author: dinangyudra@gmail.com*

(Received 14-07-2019; Revised 19-01-2020; Accepted 19-01-2020)

Abstract

Drinking water is one of the main needs of human life. Water sources do not always have the feasibility to drink. Distillation is one way to obtain potable water. Distillation can influence on drinking water quality. Low performance is a major problem in distillation. One way to improve performance is by increasing the input water temperature. One way to increase the input water temperature by utilizing heat energy on the cover glass. This study aims to improve the performance of solar energy water distillation and input water temperature by a heat exchanger. This research method is experimental. The measured variables are absorber temperature in the distillation model (T_1), glass temperature (T_2), ambient temperature (T_a), amount of distilled water produced (m) and heat energy coming from solar energy (G). This research uses variations, namely with a white or black heat exchanger and without heat exchanger. Water quality tested using 4 parameters such as microbiology, inorganic chemistry, physical and

International Journal of Applied Sciences and Smart Technologies
Volume 2, Issue 1, pages 23–34
p-ISSN 2655-8564, e-ISSN 2685-9432

chemical. Based on this study, the best results produced by a black heat exchanger using a water flow rate of $2\ l/h$ which produce distillation water $422\ ml$ ($480\ ml/(m^2.h)$) and efficiency value of 79.74%. While the best results using white heat exchanger is using $0.7\ l/hour$ water flow rate which produces distillation water of $497\ ml/(m^2.h)$) and efficiency value of 82.63%, Distilled water has increased in quality even though it has not met the standards No. 492 of 2010.

Keywords: distillation, solar energy, glass cover, water quality, efficiency.

1 Introduction

Water is one of the basic human needs that is used mainly for drinking water. Not all regions in Indonesia have water sources that are suitable for drinking, as is the case in Gunung Kidul district, Yogyakarta, which is experiencing difficulties with clean water [1]. The water sources that are often contaminated with soil, salt (seawater) or other materials. Water with these conditions can interfere with health if used directly.

Distillation is evaporation of dirty water (contaminated water) then the steam is condensed again. Steam from dirty water does not carry substances that pollute it so that the water produced from this steam condensation is feasible to drink [2].

The low performance of distillation is caused by the ineffectiveness of the evaporation and condensation process [4]. One way to increase the effectiveness of the evaporation process is to increase the temperature of the water entering the distillation. Increasing the temperature of the water entering the distillation makes the water more easily evaporated. A common way to increase the temperature of the input water is to use a solar energy water heater collector. This method requires a lot of investment costs for the manufacture of water heater collectors. In this study, another method that is cheaper and easier to use is to increase the temperature of the input water by utilizing the heat energy contained in the cover glass.

The utilization of heat energy in the cover glass is done by adding a simple heat exchanger. The heat exchanger integrated into the cover glass functions to take heat energy on the cover glass and give it to the input water. This causes the temperature of

Volume 2, Issue 1, pages 23–34
p-ISSN 2655-8564, e-ISSN 2685-9432

the input water to increase and the glass temperature to decrease. Increasing the temperature of the input water will increase the effectiveness of the evaporation process and the reduction in glass temperature will increase the effectiveness of condensation.

This study will analyze the utilization of heat energy in a cover glass to improve the performance of water distillation with solar energy. The purpose of this study is to increase the temperature of input water distillation with heat exchanger, increase the performance of the distillation of solar water by utilizing heat energy in cover glass, and to determine the quality analysis of the quality of distilled water as drinking water.

2 Research Methods

This research method is experimental. The distillation model used in indoor test includes 3 variations, white or black heat exchanger and without heat exchanger. While the variations used for outdoor include without heat exchanger and with a black heat exchanger. The input water flow rate used in indoor and outdoor research is $0.7\ l/h, 1.3\ l/h$, and $2\ l/h$. Data collection for each variation is done every 3 sunny days. Data recording is done by using sensors that are regulated by the Arduino microcontroller. In Figure 1, we can see the scheme of the tools used in this study. The main parts of this solar still include input water reservoir, heat exchanger, cover glass, absorber, non-evaporating water tank, and clean water tank.

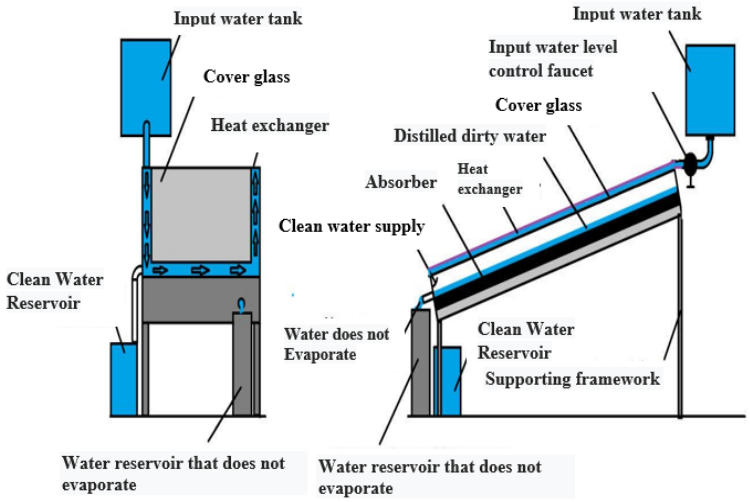


Figure 1. Parts of solar still

Volume 2, Issue 1, pages 23–34

p-ISSN 2655-8564, e-ISSN 2685-9432

For water analysis using 2 water sources, namely the source of river water and wells. Analysis of water quality carried out in the government laboratory i.e. BBTKLP is good for analysis before being distilled or after being distilled.

Data analysis used to see the performance of the distillation models used include solar energy:

$$\eta = \frac{q_e}{I(t)} \tag{1}$$

Where q_e is solar energy for the evaporation process (W/m^2) and $I(t)$ is the solar energy received by the distillation apparatus (W/m^2). The rate of evaporation is:

$$m_e = q_e/h_{fg} \tag{2}$$

Where me is the rate of evaporation of the mass of water $(kg/(s.m^2)$ and h_{fg} is the latent heat of evaporation of water (J/kg). Some heat energy is converted and radiated from glass to the environment. Constructed energy is calculated by:

$$q = h(T_1 - T_2) \tag{3}$$

Where q is convection to the environment, q_{ca} (W/m^2), h is the convection coefficient, hca $(W/m^2.{}^{O}C)$, T1 is the temperature of the glass, $T_g({}^{O}C)$ and T_2 is the ambient air temperature $({}^{O}C)$, $T_a({}^{O}C)$. Glass radiation energy into the environment is calculated using:

$$q_{ra} = \frac{\sigma[(T_1 + 273{,}15)^4 - (T_2 + 273{,}15)^4]}{\left(\frac{1}{\varepsilon_1} + \frac{1}{\varepsilon_2} - 1\right)} \tag{4}$$

Where q_{ra} is radiation to the environment, q_{ra} (W/m^2), σ is Stefan Boltzmann's $constant$ $(5.67 \times 10 - 8\, W/(m^2.K^4))$, T_1 is the glass temperature, $T_g({}^{O}C)$, T_2 is the sky temperature, T_{sky} $({}^{O}C)$, ε_1 is the emissivity of water, ε_w and ε_2 are celestial emissivity, ε_{sky} $(\varepsilon_{sky} \approx 1)$. The energy for evaporation is calculated by the equation:

$$q_e = 16{,}273 \times 10^{-3}.h_c.\left(P_w - P_g\right) \tag{5}$$

Where P_w and P_g are partial vapor pressures at water and glass temperatures. The heat energy in the cover glass that can be utilized can be calculated by the equation:

$$q_{kaca} = m.C_{p.}(T_2 - T_1) \tag{6}$$

International Journal of Applied Sciences and Smart Technologies
Volume 2, Issue 1, pages 23–34
p-ISSN 2655-8564, e-ISSN 2685-9432

Where m is the input water flow rate (kg/s), Cp is the water heat capacity ($J/(kg.^{O}C)$), T_1 is the temperature of the input water entering the heat exchanger (^{O}C) and T_2 is the temperature of the water entering the exchanger (^{O}C).

The results of the analysis of water data obtained are then evaluated by comparing the data obtained with drinking water quality requirements according to The Minister of Health Regulation No. 492 of 2010 [3]. If the data obtained meets the conditions specified by the minister of health regulations as described in the theoretical basis, distilled water qualify as drinking water and can be consumed directly.

3 Results and Discussion

The results of tools that work indoor can be seen in Figures 2, 3 and 4. In Figures 2, 3 and 4 that variations without heat exchanger are marked with brown, variations using a white heat exchanger are marked in white, and variations using a black heat exchanger are marked in black.

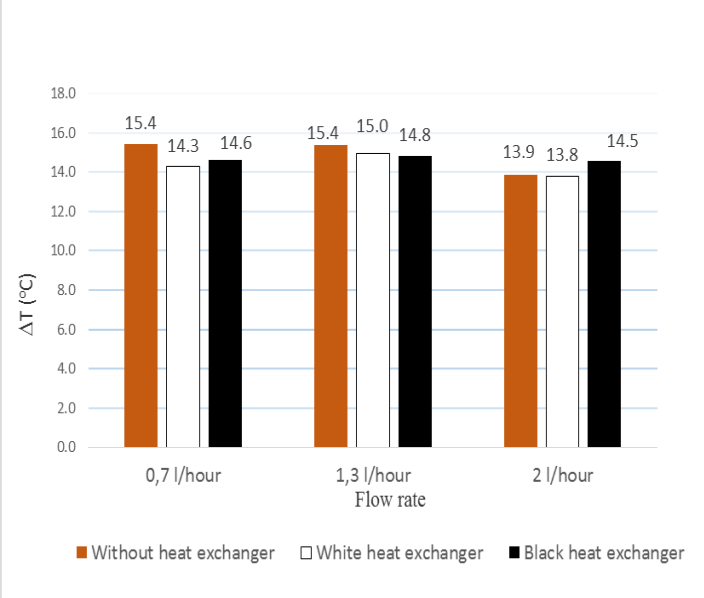


Figure 2. Graph of the average temperature difference between absorber and glass at indoor

Figure 2 is a graph of the average temperature difference (ΔT) between absorber and glass produced by various variations of water flow discharge and heat exchanger. The highest difference in temperature between the absorber and glass in the variation using

Volume 2, Issue 1, pages 23–34

p-ISSN 2655-8564, e-ISSN 2685-9432

black heat exchanger was obtained using 1.3 l/h flow rate which is 14.8 ^{O}C then followed by flow rate 0.7 l/h i.e. 14.6 ^{O}C, the lowest average temperature at 2 l/h flow rate which is 14.5 ^{O}C.

Figure 3 is a graph of the volume results generated by various variations of water flow rate and heat exchangers. The image shows the highest volume produced by the variation of the black heat exchanger using an input water flow rate of 2 l/h which is 422 ml, while the lowest volume uses input water flow rate of 1.3 $l/hour$ which is 397 ml.

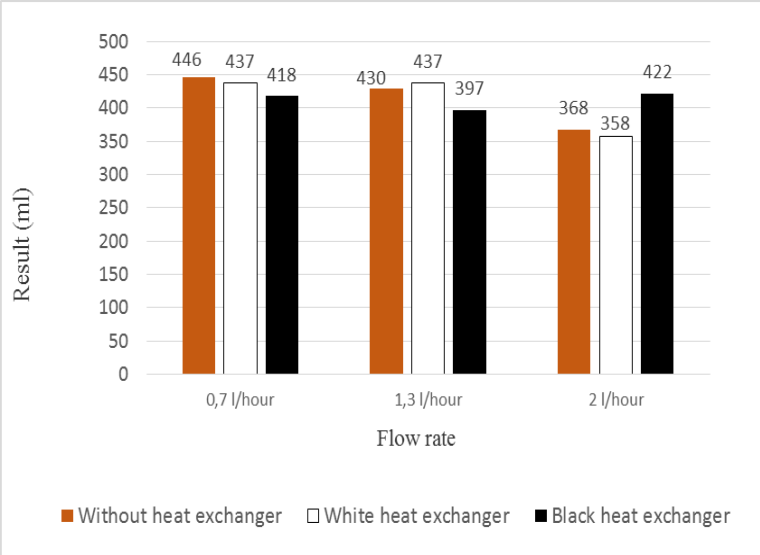


Figure 3. Graph of results of indoor distillation data

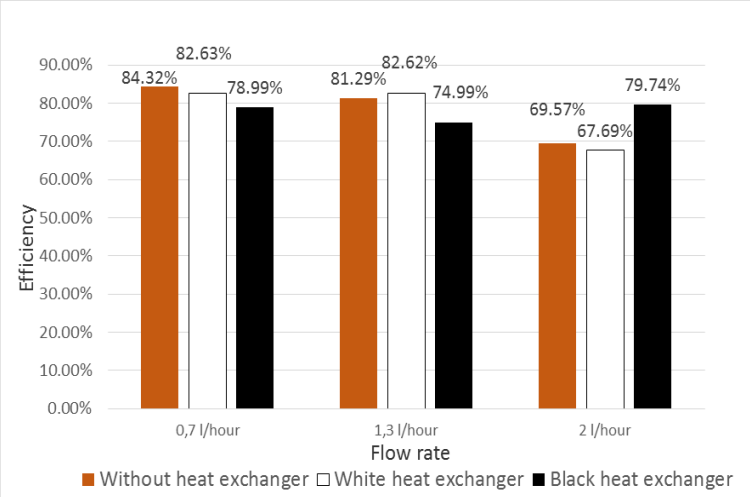


Figure 4. Indoor data collection efficiency graph

International Journal of Applied Sciences and Smart Technologies
Volume 2, Issue 1, pages 23–34
p-ISSN 2655-8564, e-ISSN 2685-9432

Figure 4 is a graph of efficiency produced by several variations of input water flow rate and heat exchanger. The graph shows the variation using a black heat exchanger which produces the highest efficiency using $2\ l/h$ water flow rate which is 79.74%. While the lowest efficiency uses 1.3 l/h water flow rate which is 74.99%.

The results of tools that work outdoors can be seen in Figures 5, 6, and 7. Outdoor data collection is carried out for 7 hours.

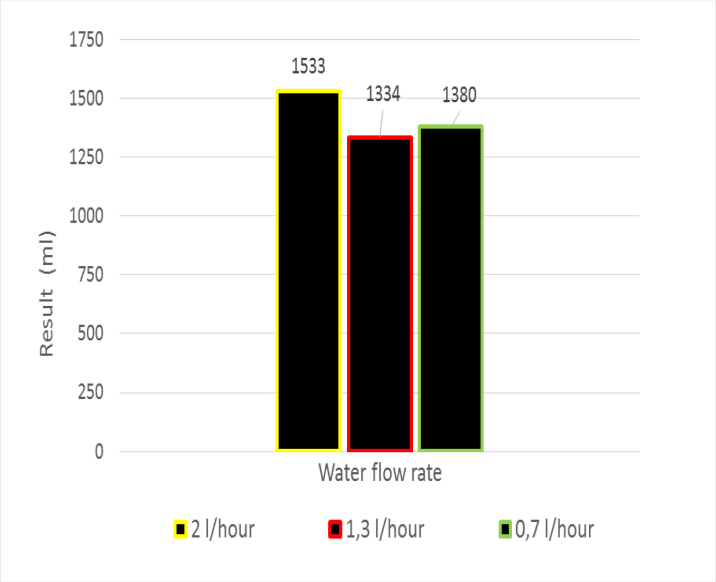


Figure 5. Graph of outdoor distillation using black heat exchanger

In Figure 5, it is known that the highest yield of black heat exchanger variations uses water flow rate $2\ l/h$ which is $1533\ ml$, while the lowest results are obtained using a 1.3 l/h water flow rate which is $1334\ ml$.

International Journal of Applied Sciences and Smart Technologies

Volume 2, Issue 1, pages 23–34

p-ISSN 2655-8564, e-ISSN 2685-9432

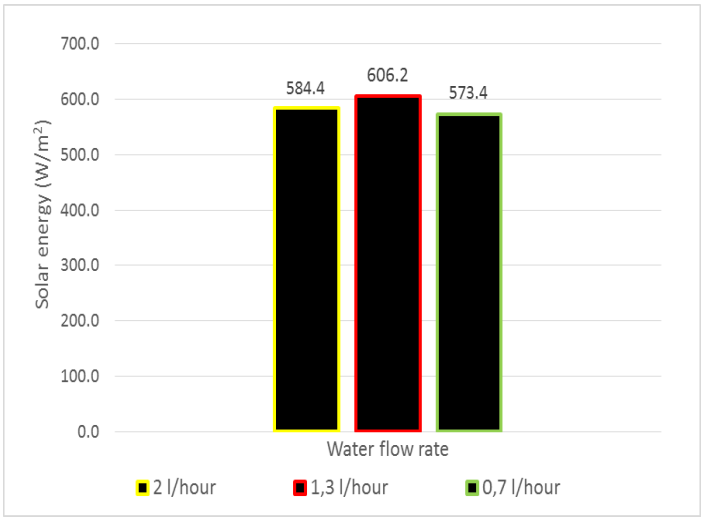


Figure 6. Average graph of the amount solar energy when taking outdoor data

Figure 6 is the average solar energy that occurs during data collection. The biggest energy occurs when the data collection uses a 1.3 l/h water flow rate reaching 606.2 W/m^2 and the smallest at 0.7 l/h water flow rate is 573.4 W/m^2.

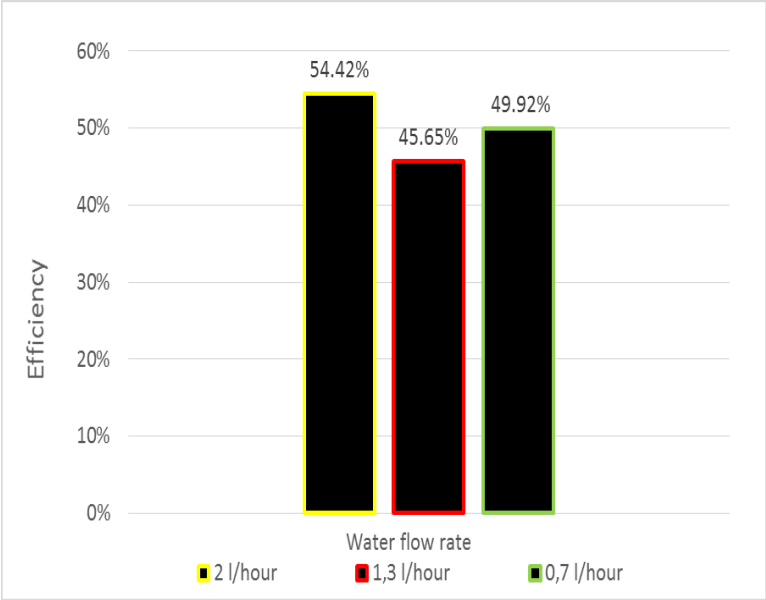


Figure 7. Graph of efficiency of the distillation tool when outdoor

Figure 7 is the efficiency produced during data collection. It can be seen that the highest efficiency is obtained at 2 l/h water flow rate, which is 54.42% and the lowest is 1.3 l/h water flow rate which is 45.65%.

International Journal of Applied Sciences and Smart Technologies

Volume 2, Issue 1, pages 23–34

p-ISSN 2655-8564, e-ISSN 2685-9432

Table 1. Standard quality of water analysis

No	Parameter	Wells Water		River Water		Maximum
		Before	After	Before	After	Level
1	Arsenic (ml/L)	$<$ 0,005	$<$ 0,005	$<$ 0,005	$<$ 0,005	0,01
2	Fluoride (ml/L)	$<$ 0,0308	$<$ 0,0308	$<$ 0,0308	$<$ 0,0308	1,5
3	Total chromium (ml/L)	$<$ 0,0213	$<$ 0,0213	$<$ 0,0213	$<$ 0,0213	0.005
4	Cadmium (ml/L)	$<$ 0,0004	$<$ 0,0004	$<$ 0,0004	$<$ 0,0004	0,003
5	Nitrite (ml/L)	$<$ 0,0013	0,0015	0,0033	$<$ 0,0013	3
6	Nitrate (ml/L)	10,85	1,24	8,54	1,24	50
7	Cyanide (ml/L)	$<$ 0,0070	$<$ 0,0070	$<$ 0,0070	$<$ 0,0070	0,07
8	Selenium (ml/L)	0,0067	0,0062	0,0010	0,0015	0,01
9	Iron (ml/L)	0,1230	0,1037	0,1230	0,1134	0,03
10	Hardness (ml/L)	165,00	5,00	192,00	3,00	500
11	Chloride	15,1	$<$ 0,6	15,1	$<$ 0,6	250
12	Manganese (ml/L)	$<$ 0,0101	$<$ 0,0101	$<$ 0,0101	$<$ 0,0101	0,4
13	pH	6,8	7,1	6,5	7,1	$6{,}5 - 8{,}5$
14	Zinc (ml/L)	$<$ 0,0083	$<$ 0,0165	$<$ 0,0083	$<$ 0,0233	3
15	Sulphate (ml/L)	28	5	16	5	250
16	Copper (ml/L)	$<$ 0,0069	$<$ 0,0069	$<$ 0,0069	$<$ 0,0069	2
17	Ammonia (ml/L)	$<$ 0,0003	$<$ 0,0003	$<$ 0,0003	$<$ 0,0003	1,5
18	Nickel (ml/L)	$<$ 0,0130	$<$ 0,0130	$<$ 0,0130	$<$ 0,0130	0,07
19	Sodium (ml/L)	14	2	15	2	200
20	Chlorine (ml/L)	$<$ 0,03	$<$ 0,03	0,05	$<$ 0,03	5
21	Lead (ml/L)	0,0058	0,0017	$<$ 0,0008	0,0011	0,01
22	Organic matter (ml/L)	1,84	0,61	2,77	1,23	10
23	Detergent (ml/L)	0,1498	0,0002	0,0219	0,1588	0,05
24	Aroma	No	No	No	No	No
25	Color (TCU)	1	$<$ 1	1	$<$ 1	15
26	TDS (ml/L)	293	23	310	10	500
27	Turbidity (MTU)	0,4	0,3	1,8	0,4	5
28	Taste	No	No	No	No	No
29	Temperature (^{O}C)	26	37	27	37	water temperature ± 3
30	E.coli (CCFU/100ml)	0	0	0	0	0
31	Total coliform	23	6	TNTC	3	0

Volume 2, Issue 1, pages 23–34
p-ISSN 2655-8564, e-ISSN 2685-9432

For the results of testing the water quality standards can be seen in Table 1, that wells and rivers that have been distilled have not met drinking water quality standards according to The Minister of Health Regulation No. 492 of 2010. The wells and rivers after being distilled have decreased and increased levels of physical and chemical and microbiological water. Decreased levels of physical, chemical and biological wells after distillation occur in the nitrate, selenium, iron, hardness, chloride, sulfate, sodium, lead, organic matter, detergent, color, TDS, coliform and turbidity. Whereas in river water there is a decrease in nitrite, nitrate, iron, hardness, chloride, sulfate, sodium, organic matter, chlorine, color, TDS, coliform, pH, temperature, and turbidity. The increase in the chemical content of distilled well water occurs in the nitrite pH, temperature and zinc content. While the distillation of river water has increased levels of zinc, selenium, lead, and detergent.

Basically water after being distilled decreases the physical and biological levels of chemicals contained in water. in this study, the increase in chemical content in water can occur due to human error or contamination by the equipment used. Even though there was an increase in the chemical content contained in well water and river water some of the contents still included drinking water quality standards except detergent in river water. Some of the contents have decreased levels of physical, chemical and biological decline, making some of the content into the drinking water quality standard.

4 Conclusion

From the results of this study, some conclusions can be obtained, including:

1. The highest water volume is obtained using a black heat exchanger at a flow rate of 2 l/h i.e 1533 ml.
2. The highest efficiency is obtained by using a black heat exchanger at a flow rate of 2 l/h i.e 54.42%.
3. Wells and river water after being distilled have better quality even though they have not met the standards of quality of the Permenkes No. 492 of 2010.

International Journal of Applied Sciences and Smart Technologies

Volume 2, Issue 1, pages 23–34

p-ISSN 2655-8564, e-ISSN 2685-9432

Acknowledgements

Thank you to the Ministry of Research, Technology, and Higher Education of the Republic of Indonesia for financing this research.

References

[1] Metrotvnews, *Kabupaten Gunung Kidul Krisis Air Bersih*. Jakarta: Metrotvnews. 2017.

[2] H. Effendi. *Telaah Kualitas Air Bagi Pengelolaan sumber Daya dan Lingkungan Perairan*. Yogyakarta: Kanisius. 2003.

[3] D. Purwodianto, FA. Rusdi Sambada,"Unjuk Kerja Destilasi Air Energi Surya Menggunakan Kondenser Pasif ," *Jurnal Penelitian*, **17** (1), 34−41, 2013.

[4] http://www.airminum.or.id/permenkes-4922010-persyaratan-kualitas-air-minum.html (Accessed on 22-10-2019).

International Journal of Applied Sciences and Smart Technologies

Volume 2, Issue 1, pages 23–34

p-ISSN 2655-8564, e-ISSN 2685-9432

This page intentionally left blank

International Journal of Applied Sciences and Smart Technologies

Volume 2, Issue 1, pages 35–44

p-ISSN 2655-8564, e-ISSN 2685-9432

A Study of Statics on Driyarkara Electric Automobile Chassis Prototype

A. H. Astyanto[1,*], Y. R. Yanto[1], A. B. W. Adi[1]

[1]*Department of Mechanical Engineering, Sanata Dharma University, Yogyakarta, Indonesia*

[*]*Corresponding Author: achil.herma@usd.ac.id*

(Received 12-06-2019; Revised 03-02-2020; Accepted 03-02-2020)

Abstract

A design phase commonly initiates either a product invention or development. Before it continues to the fabrication steps, a modern computational, enabling a simulation study during the phase, often gives opportunity to develop its effectiveness and efficiency. Through several boundary conditions, some analytical and/or computational approaches could be determined. This paper aims to elaborate both static simulations and simple experimental tests on an electric automobile chassis prototype. An application based on finite element analysis was assessed to carry out both von Misses stresses and the nodal displacements regarding the construction and/or material strength to a static loads mode. Furthermore, an experimental based examination was also executed as a simple physical validation. The studies emphasize accepted results on von Misses stresses and nodal displacements for both simulation and experimental approaches.

Keywords: chassis statics, von misses stresses, nodal displacements, finite element.

International Journal of Applied Sciences and Smart Technologies
Volume 2, Issue 1, pages 35–44
p-ISSN 2655-8564, e-ISSN 2685-9432

1 Introduction

Electric technologies inside automobiles have become worldwide during this decade. According to several studies, it offers more benefits than the conventional technologies. Mainly, electric technologies are claimed more efficient on the fuel consumption. Some others agree that the technologies are also eco-friendly on the environmental perspectives. People are now taking more concern to develop electric technologies inside automobiles which do not pollute the fresh air, and can also minimize the sound noisy.

In accordance with those several studies related electric technologies positive aspects, Indonesian government through a particular regulation lauched the National Energy Resources General Plan, called RUEN in 2017 [1]. In the regulation mentioned, sustain developments on electric automobile technologies are fully supported by the government. Some incentive packages are provided by the government for both industrial sectors and educational institutions who develop the technologies consistenly [2].

Both automobile industries and higher educational institutions welcome warmly the government offering. Through several annual exhibitions such as Gaikindo Indonesia International Motor Show (GIIAS), and Indonesia International Motor Show (IIMS), some leaders in automobile industries and also higher educational institutions have offered their performances regarding electric automobile technologies through some prototypes [3, 4].

A prototype design commonly initiates product developments, including technologies in automobiles. Nowadays, parametric based on computing aided design (CAD) features inside the technologies has improved its ease and efficiency in doing engineering design projects. Furthermore, it also enables users delivering simulation studies, including statics during design phases which is available on computing aided engineering (CAE) packages. The solution commonly involves a finite element analysis based computational methodology [5, 6].

Volume 2, Issue 1, pages 35–44
p-ISSN 2655-8564, e-ISSN 2685-9432

On a static analysis, it is also usual to conduct an experimental test through physical tests as either a comparison or validation towards the analytical/simulation results. It sometimes deals with finding the material element stresses working in the construction, namely von Misses stresses, and also the nodal displacements. Through the tests, deviations or comparisons between simulation results and physical tests can be determined. However, it can be assessed as a validation to the simulation studies [7, 8].

In this study, statics simulations based on a finite element analysis application and basic experimental tests are elaborated. The results involve von Misses stresses and nodal displacements comparison between the simulation and the experimental tests.

2 Research Methodology

Figure 1 shows the flowchart of this research. Several chassis designs by a CAD application initiated the research milestones. Some optional designs were taking into considerations during the phase. It remained models with various possibilities geometries in which the construction should able to support 0.7 $kilo\ newton$ (kN) of a minimum static load. Furthermore, a simple design was chosen based on the model simulation results. The optimum chassis design and the manufactured chassis built is shown by Figure 2.

Model simulations were conducted by a finite element analysis based application. It deals with forces acting on the construction as compensations of the real plan approaches conditions. Furthermore, results analysis involved calculations on principal stresses i.e. the maximum and minimum stresses, transformasion of plane stresses, von Misses stresses, nodal displacements and factor of safety [9].

The following step was materials preparation. Material applied in this studies is 20 $mm\ x$ 15 $mm\ x$ 1.5 $mm\ Al$ $1060-H16$ square-hollow for both the simulation and fabrication. It also dealt with some requirements regarding the maximum weight limitation of the automobile's construction. The material properties, including Young modulus, material density, the poisson ration and the yield strength of Al $1060-H16$ $a$re shown in Table 1.

International Journal of Applied Sciences and Smart Technologies

Volume 2, Issue 1, pages 35–44

p-ISSN 2655-8564, e-ISSN 2685-9432

Table 1. Material properties

Material	Elastic Modulus, MPa	Mass Density, $kg/m3$	Poisson's Ratio	Yield Strength, MPa
$Al\ 1060 - H16$	69	2705	0.33	105

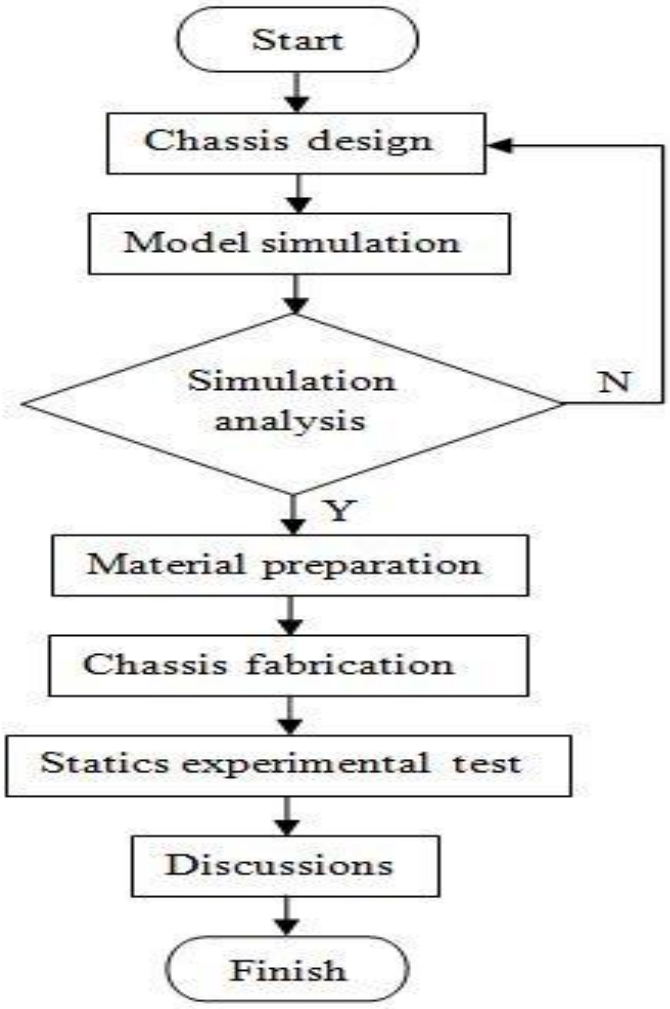


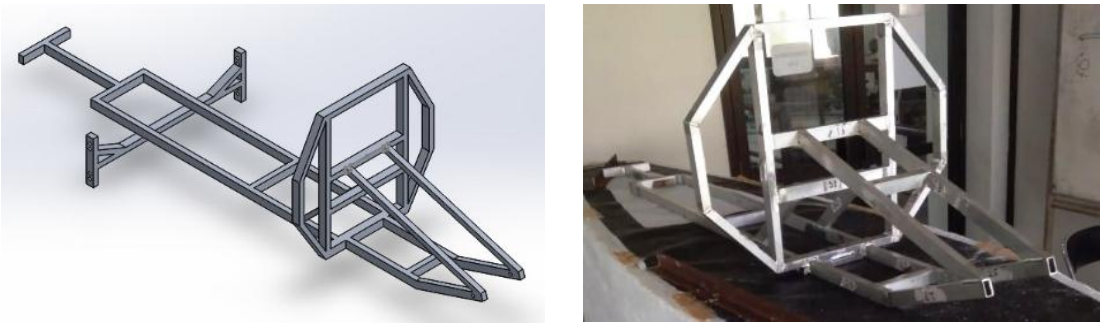
Figure 1. Flowchart of research

The chassis fabrication involved some processes of production, i.e. metal cutting and joining. It covered the processes to manufacture the geometrical shape of the chassis prototype design elected. Since the material proposed was the Aluminum, then

Volume 2, Issue 1, pages 35–44

p-ISSN 2655-8564, e-ISSN 2685-9432

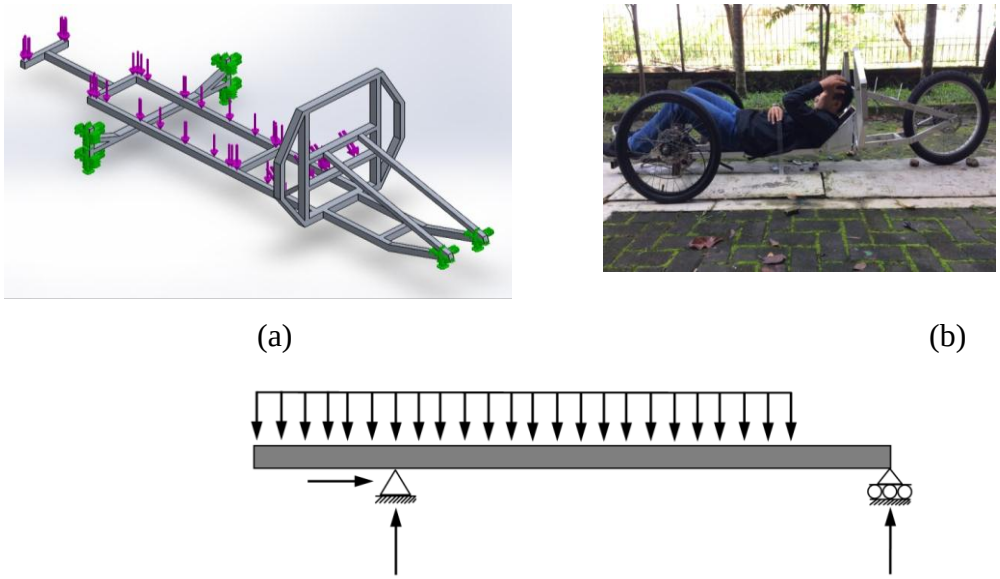
(solid metal arc welding) SMAW was applied. The global size of the chassis is $2m \times 0.5m \times 0.5m$ in length, width and heigth respectively.



(a) (b)

Figure 2. (a) Chassis prototype design and (b) after fabricated construction

Statics simulation usually requires a comparison as a physical validation. In a construction phase of developing an automobile chassis, it deals with a particular mechanics of materials approach namely forces acting in a solid body. However, the forces acting and particular strength of the construction should be determined in accordance with the properties of material strength such as the yield and ultimate strenghts. We can see on Figure 3.



(a) (b)

Figure 3. (a) Simulation boundary conditions, (b) Actual loading condition, and (c) Analytical calculation approach

International Journal of Applied Sciences and Smart Technologies

Volume 2, Issue 1, pages 35–44

p-ISSN 2655-8564, e-ISSN 2685-9432

A chassis in automobiles is a particular construction frame in which the loads of all components including the driver or passanger's weight are received and distributed. The Newton first law, involving forces acting on a solid body, states that the forces resultant of a moving body increases linearly with the acceleration, and formulated as:

$$\sum F = ma \tag{1}$$

Meanwhile, a normal stress, defined as normal force per unit area, is formulated as:

$$\sigma_{x,y} = \frac{F_n}{A} \tag{2}$$

Principal stresses, which consists of maximum and minimum stresses, are derived by transforming applied stresses as plane stresses and formulated as:

$$\sigma_{max.min} = \frac{\sigma_x + \sigma_y}{2} \pm \sqrt{\left(\frac{\sigma_x + \sigma_y}{2}\right)^2 + \tau_{xy}^2} \tag{3}$$

The safety factor emphasizes the ratio between material yield strength to applied stresses and formulated as:

$$FS = \frac{\sigma_y}{\sqrt{\sigma_a^2 - \sigma_a \sigma_b - \sigma_b^2}} \tag{4}$$

Here are in the equations:

F_n : is the normal force acting on the body

σ_Y : is the material yield strength

σ_b and σ_a : are the applied principal stresses

τ_{xy} : is the plane shear stress.

3 Results and Discussions

Figure 4 describes load vectors, von Misses stresses, and analytical space diagram as an approach to the factual condition. On the other hand, Figure 5 shows the nodal displacements on the chassis as a result of several applied load magnitudes. It deals with the boundary conditions applied as an approach on the simulation analysis. The red color indicates nodals/places with the higher impact. From the simulation results, it shows that the maximum von Misses stress on the chassis reaches up to a magnitude of

Volume 2, Issue 1, pages 35–44

p-ISSN 2655-8564, e-ISSN 2685-9432

16 MPa by applying the required load 0.76 kN of force. Meanwhile, the maximum nodal displacement on that required load reaches up to 1.42 mm by applying the equivalent force.

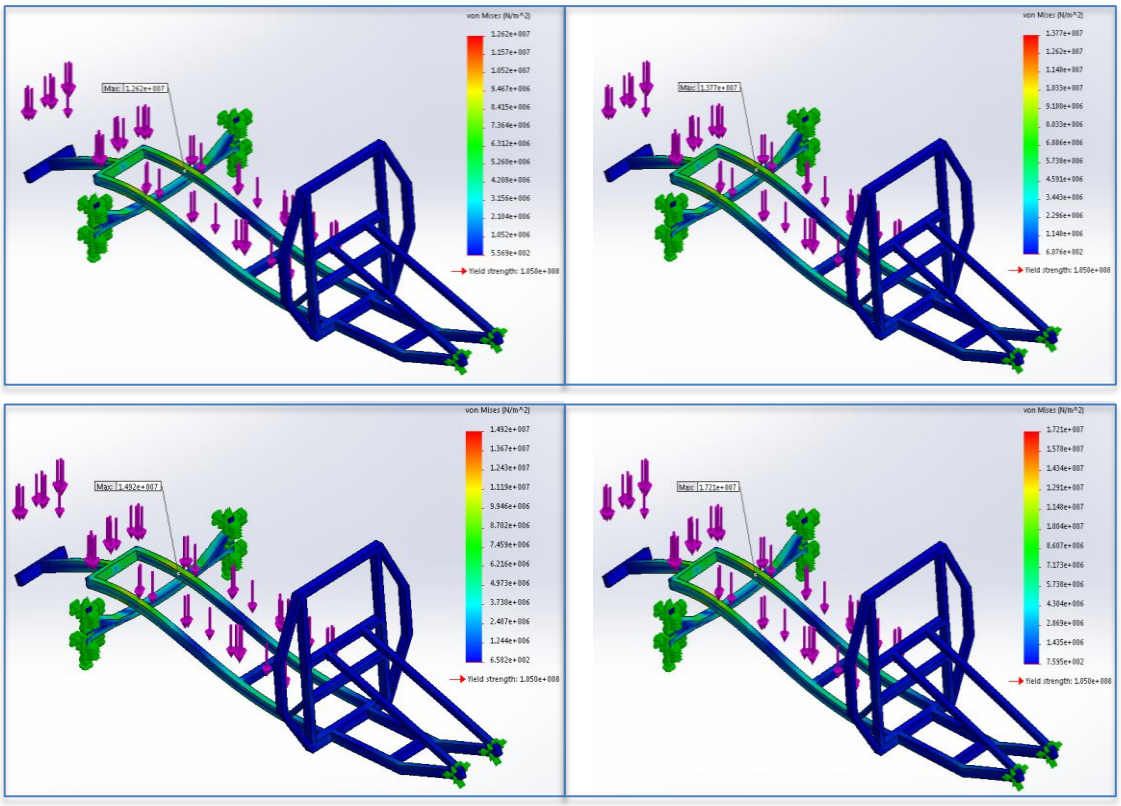


Figure 4. Von Misses Stresses distribution acting on the chassis

It is usual to reach an identification of deformation through visual observation on the chassis conditions [8]. Table 2 describes load simulation and experimental results on the maximum nodal displacements in accordance with some visual observations during several loading conditions of the chassis. On applied loads 0.50, 0.6 and 0.76 kN of forces, respectively, it shows that there are acceptable criterion between the simulation and experimental results.

International Journal of Applied Sciences and Smart Technologies

Volume 2, Issue 1, pages 35–44

p-ISSN 2655-8564, e-ISSN 2685-9432

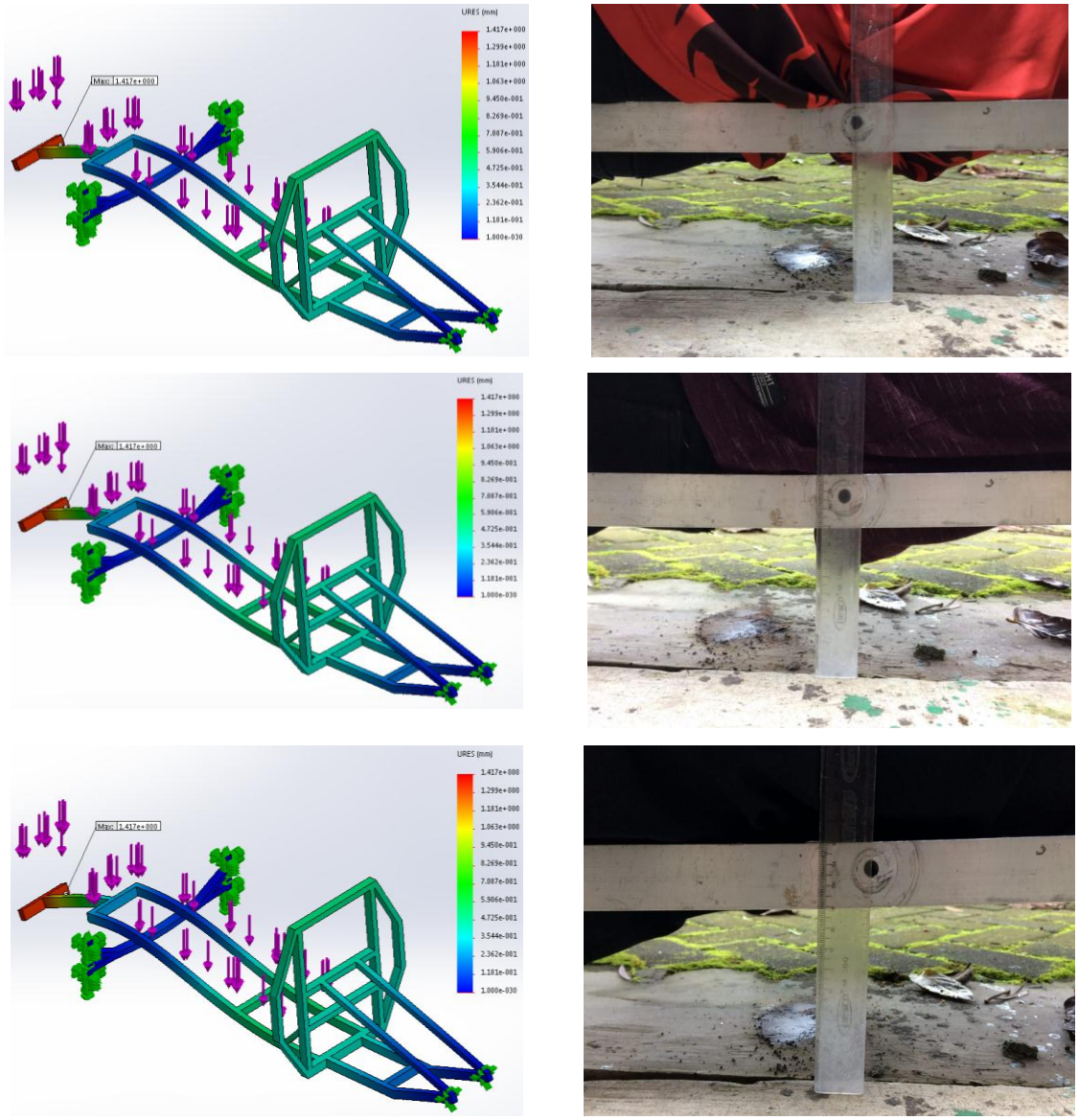


Figure 5. Nodal displacements distribution on the chassis

Table 2. Experimental visual observation

Applied load		Experimental visual observation			
kg	kN	Bending	Cracking	Fracture	Deformation
50	0.50	No	No	No	No
57	0.57	No	No	No	No
79.5	0.79	No	No	No	No

Volume 2, Issue 1, pages 35–44
p-ISSN 2655-8564, e-ISSN 2685-9432

4 Conclusions

Statics studies of an electric automobile chassis prototype have been presented on this paper. The results emphasize accepted deviations between simulation and experimental studies. On the required applied load of $0.76\ kN$ force, simulation studies show that the maximum von Misses stress and nodal displacement reach up to 0.48 MPa and $2.5\ mm$, respectively. These results describe that the material used, i.e. $Al\ 1060 - H16$ with 105 MPa of yield strength, for the construction is on the acceptable criteria. On the other hand, the experimental tests show that applying loads do not deform the chassis construction. However, optimization studies are still pursued as further developments in accordance with both the chassis design shapes/geometries and material selection. Furthermore, dynamic and lateral loads are proposed to be calculated particularly on the chassis design.

Acknowledgements

The authors would like to acknowledge the Institution of Research and Community Service (LPPM) Sanata Dharma University for the funding of these studies.

References

[1] https://www.cnbcindonesia.com/news/20180224120933-4-5336/dukung-penuh-mobil-listrik-sri-mulyani-siapkan-insentif (Accessed on 19-02-2018).

[2] https://www.cnbcindonesia.com/news/20180224120933-4-5336/menanti-insentif-mobil-listrik-di-tanah-air (Accessed on 24-02-2018).

[3] https://otomotif.kompas.com/read/2018/04/03/182200315/festival-mobil-listrik-akan-meriahkan-iims-2018 (Accessed on 11-03-2019).

[4] https://www.oto.com/berita-mobil/giias-2018-5-mobil-listrik-hadirkan-ragam-teknologi-terdepan-21181938 (Accessed on 11-03-2019).

[5] Z. Abadi, Fauzun, and M. Mahardika, "Analisa tegangan pada desain frame automatic guided vehicles (AGV) dengan pembebanan statis menggunakan

Volume 2, Issue 1, pages 35–44

p-ISSN 2655-8564, e-ISSN 2685-9432

software abaqus 6.11," *Proceeding Seminar Nasional Teknik Mesin ke-9 (SNTM 9)*, D51−D54, Agustus 2014.

[6] J. S. Pribadi, Fauzun, and M. Mahardika, "Analisa komponen kristis pada desain automatic guided vehicles (AGV) Subsystem lifting dengan pembebanan statis menggunakan software abaqus 6.11*," Proceeding Seminar Nasional Teknik Mesin ke-9 (SNTM 9*), D15−D20, Agustus 2014.

[7] M. Yamin, D. Satyadarma, and O. A. Hasanudin, "Analisis tegangan pada rangka mobil boogie," *Proceeding Seminar Ilmiah Nasional Komputer dan Sistem Intelijen (KOMMIT)*, 49−56, Agustus 2018.

[8] N. Wahyudi and Y. A. Fahrudi, "Studi eksperimen rancang bangun rangka jenis ladder frame pada kendaraan sport," *Journal of Electrical Electronic Control and Automotive Engineering*, **1** (1), 71−74, 2016.

[9] F. P. Beer, E. R. Johnston, J. T. DeWolf, and D. F. Mazurek, Mechanics of Materials, Sixth Ed, McGraw-Hill Publishing Company, New York, USA, 2012.

International Journal of Applied Sciences and Smart Technologies

Volume 2, Issue 1, pages 45–58

p-ISSN 2655-8564, e-ISSN 2685-9432

Area Under the Curves, Volume of Rotated, and Surface Area Rotated About Slanted Line

Billy Suandito

Department of Primary Teacher Education, Musi Charitas Catholic University, Palembang, Indonesia
Corresponding Author: billy_s@ukmc.ac.id

(Received 29-06-2019; Revised 05-08-2019; Accepted 05-08-2019)

Abstract

In Calculus, a definite integral can be used to calculate the area between curves and coordinate axes at certain intervals; surface area and volume formed if an area is rotated against the coordinate axis. Problems arise if you want to calculate the area of the area bounded by a curve and a line that does not form an angle of 00 or 900 to the coordinate axis, as well as the calculation of the volume of objects and the surface area of a revolution axis of rotation is a slanted line. By using existing definitions, a formula is developed for this purpose. This paper produces a finished formula, to make it easier for calculus users who do not want to know the origin method. The method used is only the method commonly used. What's new is that this formula hasn't been published in tertiary institutions or universities in Indonesia.

Keywords: the area under the curve, the volume of the rotating object, the surface area of the rotating object, the slanted line axis

International Journal of Applied Sciences and Smart Technologies

Volume 2, Issue 1, pages 45–58

p-ISSN 2655-8564, e-ISSN 2685-9432

1 Introduction

Mathematics is one of the subjects given to students from elementary school to university. One part of Mathematics is Calculus. Calculus has been given since high school to university, especially the Study Program related to Mathematics and Science. Discussion on Calculus consists of functions, limits, derivatives, derivative applications, anti-derivatives, indeterminate integrals, application of definite integrals, and integration techniques [3].

Integral is one of the sciences in the field of mathematical analysis that continues to grow rapidly, both theoretically and its applications. The application of the integral includes calculating the area of the average, the volume of the rotating object, and the area of the rotating surface. The volume of the rotating object and the swivel surface area is obtained by rotating the area of the flat plane rotated on a rotary axis [6].

Using the theory of calculating the area bounded by curves, x axis or y axis in interval $[a, b]$, commonly studied in Calculus, likewise the volume of a rotating object occurs if a curve is rotated 360^0 against the x axis or y axis, or the surface area of an object that occurs when an area is rotated against the x axis or y axis [1,3]. Problems arise, if we want to calculate the area under the curve and a sloping straight line, that is the line that forms an angle β to the positive x axis with $0^\circ < \beta < 90^0$, the area of the rotating object and the volume of the rotary object if an area is rotated against a slanted line as shown in Figure 1 [4,6].

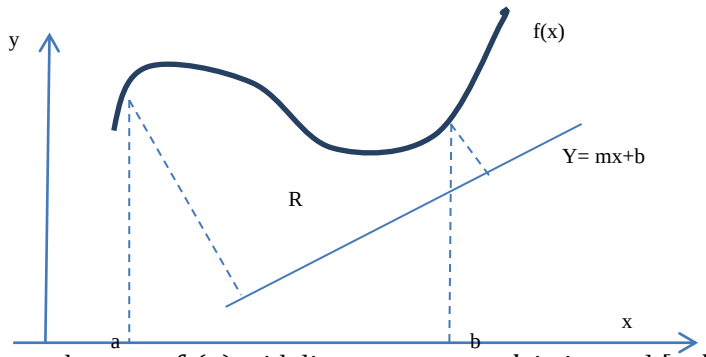


Figure 1. Area-area between $f\ (x)$ with line $y\ =\ mx\ +\ b$ in interval $[a, b]$

International Journal of Applied Sciences and Smart Technologies
Volume 2, Issue 1, pages 45–58
p-ISSN 2655-8564, e-ISSN 2685-9432

This paper is intended to formulate a formula to calculate the area under a curve, the volume of a rotating object, and the area of a rotating object against a slanted line. The position of this paper is complementary to the existing one and also to make it easier for calculus users to calculate the area under the curve up to the slanted line, the surface area of the rotating object against the slanted line, and the volume of the rotating object towards the slanted line.

2 Research Methodology

Following are a few things to keep in mind in coding equations for submission to This article is a literature review. The steps of writing are as follows

1. Reviewing Calculus textbooks, Purcell, Thomas, and James Stewart, an inseparable part of the application to calculate the area under the curve until one of the coordinate curves, rotating objects that occur when rotated in the area passed by the coordinates.
2. From Purcell, Thomas, and James Stewart's books, only in James Stewart's book found an assignment to determine the area under the curve towards the slanted line.
3. From this, developed to determine the surface area and volume that occurs if the area is rotated 3600 towards the slanted line.
4. Subsequently tested on students participating in the Calculus class majoring in Industrial Engineering and Information Engineering.

Due to time constraints, this article only contains additions to calculate the area under the curve of a slanted line, surface area and volume of objects that occur, if there is an area rotated 3600 towards a slanted line.

3 Results and Discussions

By using Integral Calculus we can calculate the area as in Figure 2. Note the area R as shown by Figure 2. The region R is bound by the x axis, the lines $x = a$ and $x = b$, and the curve having the equation $y = f(x)$, with f a continuous function at a closed

International Journal of Applied Sciences and Smart Technologies

Volume 2, Issue 1, pages 45–58

p-ISSN 2655-8564, e-ISSN 2685-9432

interval $[a, b]$. To easily fetch $x\ (x) > 0$, for all x in $[a, b]$. We will assign a value of A as the size of R.

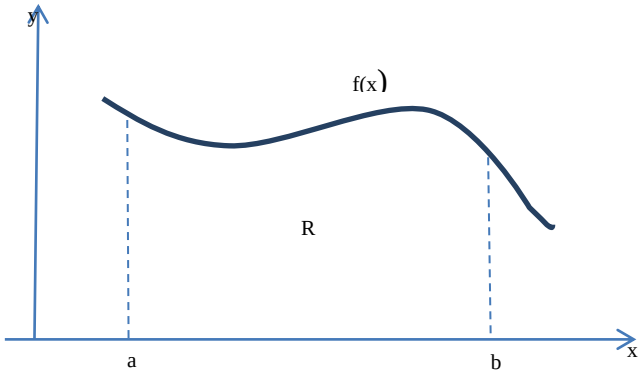


Figure 2. Area under the curve until the x axis

Firstly specify the polygon area in R. The closed hose $[a, b]$ is divided into n part of the interval of the part. To make it easier, each section hose has the same length, for example Δx. So $\Delta x = (b - a)/n$. State the endpoint of each of these intervals by $x_1, x_2, x_3, x_4, \dots, x_n$; with $x_0 = a$, $x_1 = a + \Delta x$; $x_2 = a + 2$. $\Delta x, \dots, x_i = a + i.\Delta x, \dots, x_n = a + (n).\Delta x = b$. Name the first part of the hose expressed by $[x_{i-1}, x_i]$ since continuous f function at closed hose $[a, b]$ then f continuously at each part interval [2].

According to the extreme value theorem, there is a number in each interval, at that point f reaches the absolute minimum. Suppose that in the interval the $i - th$ part of this number is c_1 such that $f(c_1)$ is the absolute minimum value of f in the interval section $[x_{i-1}, x_i]$. Note n rectangular pieces, each of which has a width of Δx unit length and height $f(c_1)$ unit length. Suppose Sn area unit states the total area of n rectangular pieces, then:

$$S_n = f(c_1).\Delta x + f(c_2).\Delta x + \cdots + f(c_i).\Delta x + \cdots + f(c_n).\Delta x$$

or

$$S_n = \sum_{i=1}^{n} f(c_i)\,.\Delta x$$

Volume 2, Issue 1, pages 45–58
p-ISSN 2655-8564, e-ISSN 2685-9432

Addition to the right hand side of the formula above gives the area of n rectangles.

Definition 1 :

Suppose the function f is continuous in the closed $interval$ $[a,b]$, with $f(x) > 0$ for each $x\ in\ [a,b]$, and that R is the area bounded by the curve $y = f(x)$, x axis, and lines $x = a$ and $x = b$. The hose $[a,b]$ is divided into n interval pieces, each in length $= (b-a)/n$; and the interval of the second part is expressed by $[x_{i-1}, x_i]$ $f(c_1)$ is the absolute minimum value of the function in the interval part i, the size of area R is given by [5]

$$A = \lim_{n\to\sim} \sum_{i=1}^{n} f(c_i)\,.\,\Delta x$$

Definition 2 :

If f is a function defined in the closed interval $[a,b]$ then certain integrals f from $a-b$, $\int_a^b f(x)dx$ are give by $\int_a^b f(x)dx = \lim_{\Delta x\to 0} f(x_i)$, if the limit exists.

Definition 3 :

Suppose the function f is continuous in the closed interval $[a,b]$, with $f(x) > 0$ for each x in $[a,b]$, and that R is the area bounded by the curve $y = f(x)$, x axis, and lines $x = a$ and $x = b$, then size A of area R is given by:

$$A = \int_a^b f(x)dx = \lim_{\Delta x\to 0} f(x_i)\Delta x$$

Suppose the function f is continuous at the closed interval $[a,b]$ with $f > 0$ for each x in $[a,b]$, and that R is a solid object obtained by rotating the area bounded by the curve $y = f(x)$, the x axis, and the lines $x = a$ and $x = b$ with respect to the x axis, then the size V is the volume of area R given by

$$V = \pi \int_a^b f(x)^2 dx = \lim_{\Delta x\to 0} \sum_{i=a}^{n} nf\,(x_i)^2 \Delta x$$

International Journal of Applied Sciences and Smart Technologies

Volume 2, Issue 1, pages 45–58

p-ISSN 2655-8564, e-ISSN 2685-9432

Definition 4 :

Suppose the function f is continuous on the closed interval $[a, b]$, with $f(x) > 0$ for each x in $[a, b]$, and that R is the surface obtained by rotating 3600 regions which are limited by the curve $y = f(x)$, x axis, and lines $x = a$ and $x = b$ with respect to x axis, then size A from area R is given by [7] :

$$A = 2\pi \int_a^b f(x)ds = \lim_{\Delta x \to 0} \sum_{i=a}^{n} 2\pi f(x_i)\Delta s$$

From the above definitions, starting discussion with including Area under the curve until the slanted line, surface area of rotating objects 360^0 against the slanted line , and volume of rotating objects 360^0 against the slanted line.

a. Area under the curve until the slanted line $y = mx + b$, as shown in Figure 3:

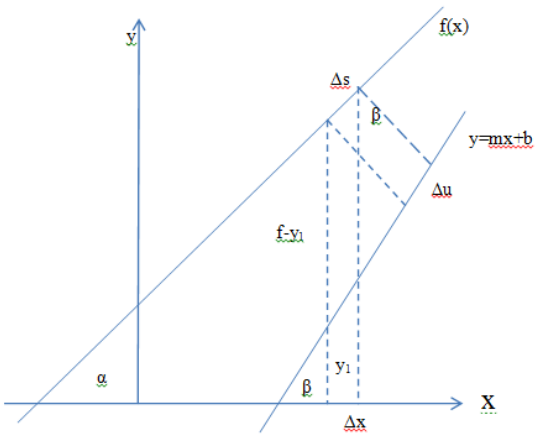


Figure 3. Small pieces perpendicular to the line $y = mx + b$

Take the area around , Δs, enlarged like Figure 4

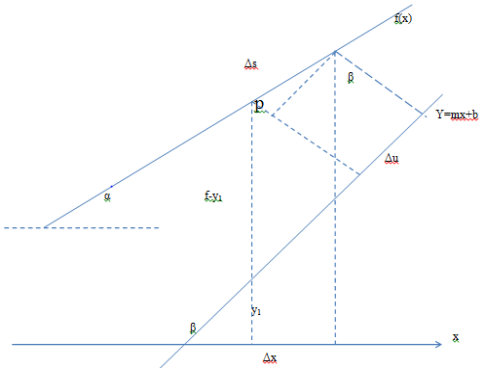


Figure 4. Section of the rectangle area Δu

International Journal of Applied Sciences and Smart Technologies

Volume 2, Issue 1, pages 45–58

p-ISSN 2655-8564, e-ISSN 2685-9432

Angle $p = 90^0 + \alpha - \beta so\ \sin\ (90^0 + \alpha - \beta) = \frac{\Delta u}{\Delta s}$, if $\sin\ (90^0 + \alpha - \beta) = \cos\ (\alpha - \beta)$, then

$$\Delta s = \frac{\Delta u}{\cos(\alpha - \beta)} \tag{1}$$

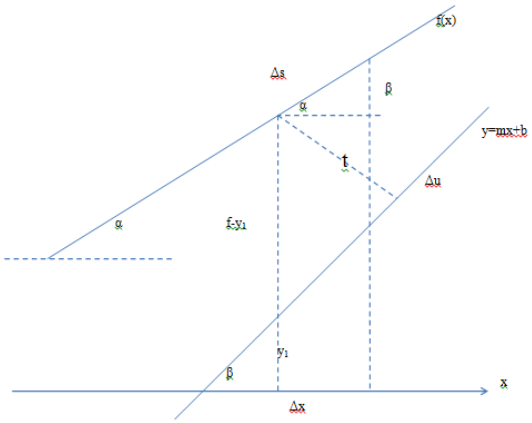


Figure 5. The area around Δu is enlarged

From Figure 5,

$$\cos\alpha = \frac{\Delta x}{\Delta s} \tag{2}$$

Subtituted (1) to (2), we get

$$\Delta u = \Delta x.\frac{\cos(\alpha - \beta)}{\cos\alpha} \tag{3}$$

Because $\cos(\alpha - \beta) = \cos\alpha.\cos\beta + \sin\alpha.\sin\beta$ so (3) become

$$\Delta u = \Delta x.\frac{cos\,\alpha.cos\,\beta + sin\,\alpha.sin\,\beta}{cos\,\alpha}$$

$$\Delta u = \Delta x.\{\cos\beta + \tan\alpha.\sin\beta\}$$

$$\Delta u = \Delta x.\cos\beta.\{1 + \tan\alpha.\tan\beta\} \tag{4}$$

Volume 2, Issue 1, pages 45–58
p-ISSN 2655-8564, e-ISSN 2685-9432

Hence $\tan \alpha$ is a gradient of tangent, then $\tan \alpha = f'$ and $\tan \beta = m$ so (4) become

$$\Delta u = \Delta x . \cos \beta [1 + f' . m] \quad (5)$$

From Figure 5, $\cos \beta = \frac{1}{f - y_1}$ or

$$t = (f - y_1) . \cos \beta \quad (6)$$

If $\Delta A = t . \Delta u$, then subtitued (5) and (6) get

$$\Delta A = (f - y_1) . cos\, \beta \, . \Delta x \, [1 + f' . m]$$
$$\Delta A = (f - y_1) . cos^2 \beta \, [1 + f' . m] . \Delta x .$$

Because $cos^2 \beta = \frac{1}{1 + tan^2 \beta}$ and $\tan \beta = m$, so

$$\Delta A = (f - y_1) . \frac{1}{1 + m^2} . [1 + f' . m] . \Delta x .$$

From definition are we get

$$A = \int_a^b \frac{1}{1 + m^2} . (f - y_1) . [1 + f' . m] dx \quad (7)$$

This formula use for calculate area the curve until the slanted line.

b. Area of Rotating Objects Against The Slanted Line

If the slice Δs is rotated 360^0 against the line $y = mx + b$, a thin cylinder is formed with t as the radius and Δs as the height, so that the surface area is

$$\Delta A = 2\pi . t . \Delta s$$

With subtitute (2) , (6), $\cos \beta = \sqrt{\frac{1}{1 + m^2}}$ and $\cos \alpha = \frac{1}{\sqrt{1 + (f')^2}}$ get

$$A = \int_a^b \frac{2\pi}{\sqrt{1 + m^2}} (f - y_1) . \sqrt{1 + (f')^2} \, dx \quad (8)$$

This formula is used for calculate area of rotating 360^0 against the slanted line.

International Journal of Applied Sciences and Smart Technologies

Volume 2, Issue 1, pages 45–58

p-ISSN 2655-8564, e-ISSN 2685-9432

c. Volume of Rotating Objects

Now discuss for to get formula of volume of rotating objects 360^0 against the slanted line. If the slice Δs is rotated 360^0 against the line $y = mx + b$, it will form a thin cylinder with t as the radius and Δu as the height, so the volume is

$$\Delta V = \pi . t^2 . \Delta u$$

With subtitued (4), (6) , and $cos\,\beta = \sqrt{\frac{1}{1+m^2}}$ get

$$\Delta V = \pi . (f - y_1)^2 . cos^3 \beta . (1 + f' . m) . \Delta x$$

and

$$V = \int_a^b \frac{\pi}{(1+m^2)^{\frac{3}{2}}} (f - y_1)^2 . (1 + f\text{^}' . m) dx \tag{9}$$

This formula is used for calculate volume of rotating 360^0 against the slanted line.

d. Example

Now for example, the area will be determined by the line AB, as shown in Figure 6. The line $y = 2x + 3$ and the line perpendicular to $y = 2x + 3$ drawn from point $(1,8)$ and $B\ (3,10)$.

Solution:

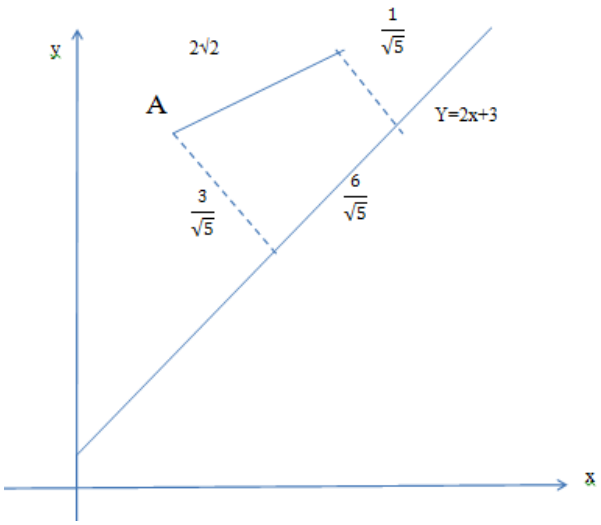


Figure 6. Visualizes the sample count

Volume 2, Issue 1, pages 45–58

p-ISSN 2655-8564, e-ISSN 2685-9432

Equation of line of AB is $y = x + 7$, gradient $m = 1$, $Y = 2x + 3$ so $f' = 2$

Area counted using formula (7)

$$Area = \int_1^3 \frac{1}{1+2^2}.(x + 7 - 2x - 3).(1 + 2.1)dx$$

$$Area = \int_1^3 \frac{1}{5}.(4 - x).3dx$$

$$Area = \frac{3}{5}.\int_1^3 (4 - x)dx$$

$$Area = \frac{3}{5}.(4x - \frac{1}{2}x^2)_1^3$$

$$Area = \frac{3}{5}.[\left(4.3 - \frac{1}{2}.3^2\right) - \left(4.1 - \frac{1}{2}.1^2\right)]$$

$$Area = \frac{3}{5}.\left[12 - \frac{9}{2} - 4 + \frac{1}{2}\right] = 2{,}4$$

The form of wake occurs is trapeze with measure of edge parallel is $\frac{1}{\sqrt{5}}$ and $\frac{3}{\sqrt{5}}$ and height $\frac{6}{\sqrt{5}}$.

Area of trapeze is ½ sum of edge paralels accrossed by heightso given

$\frac{1}{2}.\left(\frac{1}{\sqrt{5}} + \frac{3}{\sqrt{5}}\right).(\frac{6}{\sqrt{5}}) = \frac{1}{2}.\frac{4}{\sqrt{5}}.\frac{6}{\sqrt{5}} = \frac{24}{10} = 2{,}4$

For the area rotated against the line $y = 2x + 3$, the object that occurs is the surface of the cone. The area can be calculated using the formula of a large cone blanket area minus the size of a small cone blanket. The cone blanket area is calculated by formula $A = \pi.r.s$

Where A is the area of a cone blanket r is the radius of the cone base s is a cone painter line (hypotenuse).

For the example of this count the large cone base radius is $\frac{3}{\sqrt{5}}$ and s is $4\sqrt{2}$ and the small cone base radius is $\frac{1}{\sqrt{5}}$ and the painter's line length is $\sqrt{2}$.

$$A = \pi.\frac{3}{\sqrt{5}}.4\sqrt{2} - \pi.\frac{1}{\sqrt{5}}.\sqrt{2} = \frac{8}{5}\pi\sqrt{10}$$

International Journal of Applied Sciences and Smart Technologies

Volume 2, Issue 1, pages 45–58

p-ISSN 2655-8564, e-ISSN 2685-9432

Using formula 8 we get

$$A = \int_1^3 \frac{2\pi}{\sqrt{1+m^2}}.(f-y_1)\sqrt{1+(f')^2}\,dx$$

$$A = \int_1^3 \frac{2\pi}{\sqrt{1+2^2}}(x+7-2x-3).\sqrt{1+(1)^2}dx$$

$$A = \frac{2\pi\sqrt{2}}{\sqrt{5}}\int_1^3 (4-x)dx$$

$$A = \frac{2\pi\sqrt{10}}{5}.-1(4-x)^2]_1^3$$

$$A = -\frac{2\pi\sqrt{10}}{5}[(4-3)^2-(4-1)^2] = \frac{8\pi\sqrt{10}}{5}$$

While he volume of objects that occur is a cone that is stuck. Using formula $V = \frac{1}{3}\pi.r^2.t$, we count volume big cone minus volume of a little cone.

$$V = \frac{1}{3}\pi.(\frac{3}{\sqrt{5}})^2.\left(\frac{9}{\sqrt{5}}\right) - \frac{1}{3}\pi.(\frac{1}{\sqrt{5}})^2.(\frac{3}{\sqrt{5}})$$

$$V = \pi.\frac{27}{5\sqrt{5}} - \pi.\frac{1}{5\sqrt{5}}$$

$$V = \pi.\frac{26}{5\sqrt{5}}$$

Using formula 9 get

$$V = \int_1^3 \frac{\pi}{(1+2^2)^{\frac{3}{2}}}.(4-x)^2.(1+2.1)dx$$

$$V = \int_1^3 \frac{3\pi}{5\sqrt{5}}.(4-x)^2dx$$

Volume 2, Issue 1, pages 45–58

p-ISSN 2655-8564, e-ISSN 2685-9432

$$V = \frac{3\pi}{5\sqrt{5}} . -\frac{1}{3}(4-x)^3]_1^3$$

$$V = -\frac{\pi}{5\sqrt{5}} . [1^3 - 3^3]$$

$$V = \frac{26\pi}{5\sqrt{5}}$$

4 Conclusions

From the discussion of examples of counts, it can be seen that using formulas 7, 8, and 9 are not different by using the formula of flat building and space that is commonly used. Thus the area under the curve to the straight line is known not horizontally or vertically and the rotating surface area and the volume of rotary matter can be calculated using formulas (7), (8), and (9). Suggestions for future researchers, can conduct learning research, valid or not the formula.

Acknowledgements

The author would like to thank his colleagues who have helped prepare everything needed so that this paper can be realized.

References

[1] P. Ferdias, and E. A. Savitri, ”Analisis materi volume benda putar pada aplikasi cara kerja piston di mesin kendaraan roda dua”, *Jurnal Pendidikan Matematika Al-Jabar,* **6** (2), 177−182, 2015.

[2] Purcell, et al, “Calculus and Analityc Geometry”, Pearson, New Jersey, 9th edition, 2007.

[3] Y. Romadiastri, “Penerapan pembelajaran kontekstual pada kalkulus 2 bahasan volum benda putar”, *Jurnal Phenomenon*, **1** (1), 131−143, 2013.

[4] M. S. Rudiyanto dan S. B. Waluya, “Pengembangan model pembelajaran matematika volume benda putar berbasis teknologi dengan strategi konstruktivisme student active learning berbantuan cd interaktifkelas XII”,*Jurnal Matematika Kreatif-Inovatif*, **1** (1), 33−44, 2010.

Volume 2, Issue 1, pages 45–58

p-ISSN 2655-8564, e-ISSN 2685-9432

[5] J. Stewart, “Calculus”, Thomson Brooke, Beltmont, 5th edition, 2007.

[6] Sumargiyani, “Penerapan pembelajaran kontekstual pada pembahasan volume benda putar dengan pembelajaran kontekstual”, *Prosiding Seminar Nasional Matematika dan Pendidikan Matematika*, 2006.

[7] M. D. Weir, and J. Hass, ”Thomas’Calculus”, Pearson, Boston, 12th edition, 2010.

International Journal of Applied Sciences and Smart Technologies

Volume 2, Issue 1, pages 45–58

p-ISSN 2655-8564, e-ISSN 2685-9432

This page intentionally left blank

International Journal of Applied Sciences and Smart Technologies

Volume 2, Issue 1, pages 59–66

p-ISSN 2655-8564, e-ISSN 2685-9432

Comparison Simulation Analysis of the Gradual Summation of a Function with Recognition of Direct Extrapolation via IN Series

Stephanus Ivan Goenawan

Department of Industrial Engineering, Atma Jaya Catholic University,
Cisauk BSD Highway, Tangerang, Indonesia
Corresponding Author: steph.goenawan@atmajaya.ac.id

(Received 26-06-2019; Revised 05-08-2019; Accepted 05-08-2019)

Abstract

A set of data pattern that have the characteristic of a function can be approached using Newton series simulation. When using the Newton series, the simulation result of the summation of extrapolation data can be gradually done in step by step. However, if using the IN series, the simulation result of the summation of extrapolation data doesn't need to be gradually done in step by step. The methodology in this research compares the data pattern from the simulation results of the high degree function with the results of interpolation and extrapolation from the results of the IN series simulation. Furthermore, will be carried out comparison simulation analysis of the summation of the function values gradually with the extrapolation function directly using the IN series. The result of comparison simulation analysis point out that the value of the total summation of data between the gradual and the direct summation is the same, so that the direct sum technique using the IN Series is able to make the total sum process more efficient.

Keywords: IN series, Newton series, extrapolation, interpolation

International Journal of Applied Sciences and Smart Technologies

Volume 2, Issue 1, pages 59–66

p-ISSN 2655-8564, e-ISSN 2685-9432

1 Introduction

The IN series, namely Ivan Newton Series (according to HKI EC00201856522), is a further development of the Newton series [1]. A function that is built from a Newton series must have function basis which has a form $\prod_{i=0}^{n}(x-i)$, where the value of n is a positive integer [2]. If the numbers of the function that has been successfully built by the Newton series are summed gradually, of course there will be inefficient constraints because it will require repetitive summation processes carried out sequentially so that it can take longer than without the repeated summation process. Therefore the sum of extrapolation results can later be obtained in a more efficient way, so a new series has been developed, namely Ivan Newton series or abbreviated as IN series [3]. This IN series is generated from the function basis of multilevel series of j in one degree $\sum_{j=1}^{t} {}^{u+i-1}\, j$ where the values of $u, i,$ and t are positive integers. Of course if the function data is not summed, so the form of the function basis will be similar to the function basis of the Newton series. Its function base if $u = 0$ we have

$$\frac{1}{(n-1)!}\prod_{i=0}^{n}(x+i) \quad .$$

Because this function base equation has similarities and capabilities similar to the Newton series, which is able to interpolate and extrapolate the data, so this series is named Ivan Newton series.

2 Basic Theory

Before discussing the IN series, it will be explained about multilevel series of j in one degree which plays an important role as the function basis of the IN series [4]. The multilevel series of j in one degree is the series of j in one degree which is repeated again in addition, with an initial limit of one [5]. To be clearer, this below is a definition of the notation of the multilevel summation, with t and u is a positive integer, where $t \geq 1$ and $u \geq 0$.

International Journal of Applied Sciences and Smart Technologies

Volume 2, Issue 1, pages 59–66

p-ISSN 2655-8564, e-ISSN 2685-9432

$$\sum_{i=1}^{t} {}^{0}i \equiv t$$
$$\sum_{i=1}^{t} {}^{1}i \equiv \sum_{i=1}^{t} i \equiv 1+2+3+.....+t \tag{1}$$
$$\sum_{i=1}^{t} {}^{2}i \equiv \sum_{j}^{t}\sum_{i=1}^{j} i \equiv 1+(1+2)+(1+2+3)+....+(1+2+3+....+t)$$

Furthermore, in general it can be obtained [4],

$$\sum_{i=1}^{t} {}^{u}i = \binom{t+u}{u+1} \tag{2}$$

The form of the IN series [3] which uses the function basis of the multilevel series of j in one degree equation (4) is

$$\begin{aligned}\sum_{i=1}^{t} {}^{u} f(\alpha \cdot i) &\cong \sum_{l=0}^{\beta} b_l \cdot g(l,u,t) \\ &\cong b_0 \cdot g(0,u,t) + b_1 \cdot g(1,u,t) + b_2 \cdot g(2,u,t) + \\ &\quad b_3 \cdot g(3,u,t) + ... + b_\beta \cdot g(\beta,u,t).\end{aligned} \tag{3}$$

where

$$g(i,u,t) = \sum_{j=1}^{t} {}^{u+i-1} j = \binom{u+i+t-1}{u+i} \tag{4}$$

The smallest function base if the value $i = 0$ is

$$g(0,u,t) = \binom{t+u-1}{u} \tag{5}$$

In the formula of the IN series equation (3), the value of the variable t is a positive integer for value $u \geq 1$, but if $u = 0$ the the range for the variable value t changes to a real number, the formula is the same as in the Newton series. The formula form of the IN series which the results are not summed with the value $u = 0$ and the difference factor between discrete data $\alpha = 1$ in the equation (3) is

$$\begin{aligned}\sum_{i=1}^{t} {}^{0} f(i) = f(t) &\cong b_0 + b_1 \cdot t + b_2 \cdot \frac{t \cdot (t+1)}{2!} + \\ &\quad b_3 \cdot \frac{t \cdot (t+1) \cdot (t+2)}{3!} + ... + b_\beta \cdot \frac{\prod_{k=0}^{\beta-1} (t+k)}{\beta.!}.\end{aligned} \tag{6}$$

or

International Journal of Applied Sciences and Smart Technologies

Volume 2, Issue 1, pages 59–66

p-ISSN 2655-8564, e-ISSN 2685-9432

$$f(t) \cong b_0 + \sum_{j=1}^{\beta} b_j \cdot \frac{\prod_{k=0}^{j-1}(t+k)}{j!} \tag{7}$$

with the value of $b_0 = f(0)$.

By using the interpolation method of the IN series, the constants that compose the IN series equation (3) can be generated [6], that is:

$$b_0 = f(0), \qquad b_1 = -\left(f(-1) - b_0\right) \tag{8}$$

and

$$b_l = \left(\begin{array}{l} f(-l) - b_0 - b_1 \cdot (-l) - b_2 \cdot \dfrac{\prod_{k=0}^{1}(-l+k)}{2!} - b_3 \cdot \dfrac{\prod_{k=0}^{2}(-l+k)}{3!} - \\ \qquad \ldots\ldots\ldots\ldots\ldots\ldots - b_{l-1} \cdot \dfrac{\prod_{k=0}^{l-2}(-l+k)}{(l-1)!} \end{array} \right) \cdot \frac{l!}{\prod_{k=0}^{l-1}(-l+k)} \tag{9}$$

or

$$b_l = \left(f(-l) - b_0 - \sum_{j=1}^{l-1} b_j \cdot \frac{\prod_{k=0}^{j-1}(-l+k)}{(j-1)!} \right) \cdot \frac{l.!}{\prod_{k=0}^{l-1}(-l+k)} \tag{10}$$

where the value range l is positive integer numbers, $l = 2, 3, 4, \ldots$.

3 Results and Discussions

From equation (9) and (10), an algorithm for interpolation can be made using the IN series. An example of the initial polynomial data that will be used for interpolation is to find the values of constants in the IN series in Table 1 derived from the polynomial function equation (11).

The data in this Table 1 are derived from the polynomial function that will be used for the direct sum extrapolation test in the Table 3, that is:

$$f(x) = 1 + x - \frac{x^2}{2^2} + \frac{x^4}{4^4} - \frac{x^6}{7^6} - \frac{x^8}{10^8} + \frac{x^{10}}{(11.4)^{10}} \tag{11}$$

Volume 2, Issue 1, pages 59–66

p-ISSN 2655-8564, e-ISSN 2685-9432

with a range of abscissa from -22 to 22, a representation of the polynomial function can be described through Figure 1.

Table 1. Interpolation polynomial data in the IN series

t	$f(t)$
0	1
-1	-0.246
-2	-1.938
-3	-3.939
-4	-6.035
-5	-7.945
-6	-9.349
-7	-9.921
-8	-9.367
-9	-7.474
-10	-4.167
-11	0.439
-12	5.989

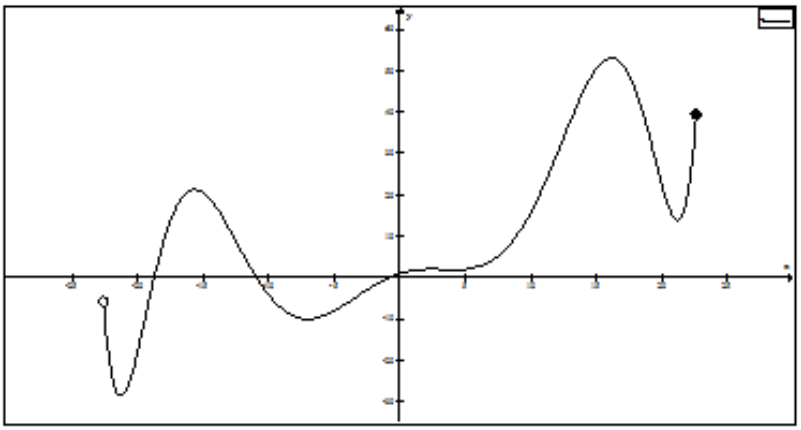


Figure 1. Graph of a polynomial function equation

After using the interpolation formula of the IN series, equation (8) and (9), can be generated the constants in each basis of the IN series function as shown in Table 2.

Volume 2, Issue 1, pages 59–66

p-ISSN 2655-8564, e-ISSN 2685-9432

Table 2. Constant values on the IN series function

n	$b(n)$
0	1
1	1.24610226
2	−0.44584200
3	−0.13597862
4	0.08010405
5	0.01642209
6	−0.00759176
7	0.00061180
8	0.00041250
9	−0.00044048
10	$9.7884E-05$
11	$-7.6206E-13$
12	$-1.7150E-12$

Generating of the IN series function can be done after the constant values in Table 2 are obtained. Then the data extrapolation test and summation are carried out, summation in level one directly from the interpolated polynomial function using the EXCEL. The results are shown in Table 3.

Table 3. Comparison test of extrapolation data and direct summation using the IN series

t	Data from the actual polynomial function $f(t)$	Gradual data summation of function $f(t)$	Ekstrapolation data using IN series	Summation of data directly using IN series
1	1.753898	1.753898	1.753898	1.753898
2	2.061953	3.815851	2.061953	3.815851
3	2.060146	5.875997	2.060146	5.875997
4	1.964557	7.840555	1.964557	7.840555
5	2.054953	9.895508	2.054953	9.895508
6	2.650765	12.54627	2.650765	12.54627
7	4.078878	16.62515	4.078878	16.62515
8	6.633004	23.25816	6.633004	23.25815
9	10.52532	33.78347	10.52532	33.78347
10	15.83238	49.61586	15.83238	49.61586
11	22.43944	72.0553	22.43944	72.0553
12	29.98992	102.0452	29.98992	102.0452
13	37.85055	139.8958	37.85054	139.8958
14	45.10707	185.0028	45.10706	185.0028
15	50.61107	**235.6139**	50.61105	**235.6139**

Volume 2, Issue 1, pages 59–66
p-ISSN 2655-8564, e-ISSN 2685-9432

After obtaining the extrapolation data, it is necessary to compare the data result with the actual polynomial function, it turns out that from Table 3 the same data results are obtained. Furthermore, it is also necessary to compare the sum results of polynomial function data one by one with the sum results directly using the IN series, it turns out that from Table 3 the same results are also obtained.

4 Conclusions

a. Ivan Newton series or IN series is a series formula that is more general than the Newton series because it is able to direct summation of extrapolation data on polynomial functions.
b. The basis of the function that compose the IN series is the multilevel series of j in one degree.
c. Interpolation simulation from IN series can be used to extrapolate data well if the data characteristic is polynomial function.
d. In the future the IN series can be utilized in numerical methods.

Acknowledgements

This work was supported by the LPPM Atma Jaya Catholic University. The author thanks the reviewers for their suggestions, which have improved the quality of this paper.

References

[1] I. Newton, “Philosophiae naturalis principia mathematica Book III,” London, 1687.
[2] R. W. Hamming, “Numerical methods for scientists and engineering: 2nd,” *Dover Publication, Inc*. New York, 1973.
[3] S. I. Goenawan, “Deret IN (Ivan Newton): formula efisien untuk jumlahan bertingkat data interpolasi atau ekstrapolasi,” HKI EC00201856522, 2018.
[4] S. I. Goenawan, “Deret bertingkat berderajat satu dalam teori keteraturan,” *Metris*, **4** (1), 50−56, 2003.

Volume 2, Issue 1, pages 59–66

p-ISSN 2655-8564, e-ISSN 2685-9432

[5] S. I. Goenawan, "Teori keteraturan," ATMA nan JAYA, Jakarta, 1998.

[6] S. I. Goenawan, "Deret garis bertingkat dalam teori keteraturan," *Metris*, **3** (3), 50−57, 2002.

International Journal of Applied Sciences and Smart Technologies

Volume 2, Issue 1, pages 67–74

p-ISSN 2655-8564, e-ISSN 2685-9432

Application of Klein-4 Group on Domino Card

Asido Saragih[1,*], Santri Chintia Purba[2]

[1]*Department of Mathematics, Satya Wacana Christian University, Salatiga, Indonesia*

[2]*Department of Educational Mathematics, Christian University of Indonesia, Jakarta, Indonesia*

[*]*Corresponding Author: saragihasido@gmail.com*

(Received 04-11-2019; Revised 03-02-2020; Accepted 03-02-2020)

Abstract

Klein-4 or Klein-V group is a group with four elements including identity. The binary operation on Klein-4 group will produce identitiy if operated to it self and produce another non-identity element if operated to another non-identity element. The focus of this paper is to explain the principle of Klein-4 group on Domino card and also find all complete possible elements. Domino card is a set of 28 cards which the surface of each card divided in two identic boxes contain combination of dots as pattern. The final part of this research is to find out all possible combination of cards which can be used as elements of a Klein-4 groups.

Keywords: klein, domino

1 Introduction

Group is a set of nonempty elements with a well define binary operation which satisfy conditions for binary operation are associative, has identity and inverse element,

Volume 2, Issue 1, pages 67–74
p-ISSN 2655-8564, e-ISSN 2685-9432

and close under binary operation [1]. We notice a group G with binary operation $*$ as $(G,*)$.

Definition 1.1.

Let $(G,*)$ be a group. Then G is an abelian group if elements of G are commutative under $*$. The name of abelian group is actually was given for honors a Norwegian mathematics Niels Hendrik Abel [2] . Further for our convenience, let us denote $\{p\}^k$ be $k-th$ repetitions of p under the operation of binary operation $*$. For example $\{p\}^2 = p * p$, and $\{p\}^4 = p * p * p * p$.

Let p and q are two numbers such that $0 \leq p \leq 6$ and $0 \leq q \leq 6$. We construct an abreviation with equivalent meaning as $0 \leq p, q \leq 6$ to help us in simplification writing.

Definition 1.2.

Let $(G,*)$ be a group, and $p, q, e \in G$, with e is the identity. We say p is generator of q if there exists a positive integer n such that $\{p\}^n = q$. In this case it is not surprise to make an understending that p generate q. Furthermore, we say a positive integer m be the order of p if $\{p\}^m = e$.

Definition 1.3.

Let $(G,*)$ be a group. Then we say G is a cyclic group if there exists an element $p \in G$ and p generate all elements of G [3].

Basically there are a lot of group we can construct. But there is one simple and interesting group named Klein-4 group which also oftenly signed as V_4 stand for *"Vier"*, means "four" in German and *"Klein"* means "small" [4]. A Klein-4 group or Klein-V group is a group with four elements including identity. Klein-4 with a binary operation $\bullet$ and e as identity, will produce e if an element operated to it self and produce it self if operated with e. If two different non-identity elements are operated by $\bullet$, will produce the another non-identity element. For example, let $(G,\bullet) = \{e, a, b, c\}$

Volume 2, Issue 1, pages 67–74

p-ISSN 2655-8564, e-ISSN 2685-9432

as a Klein-4 group. Then, the result of the operation over • represented on Table 1 below :

Table 1. Klein-4 group

•	e	a	b	c
e	e	a	b	c
a	a	e	c	b
b	b	c	e	a
c	c	b	a	e

Certainly, the simplicity concept of Klein-4 group makes it become interesting to observe. Collecting four object with a binary operation to represent Klein-4 group would not be easy to define. However, group theorists tried to find Klein-4 group applications in daily life. In order to reach that purpose, of course they need to find the generator elements to generate it. For example, Samuel and Mshelia [5] found one of the its application on a game called ”Tsorry Checkerboard” which consists of 2×2 boxes with some rule and moving code. On another side Rietman, Robert and Jack [6] explain about Klein-4 group in genetic coding. Especially for its identity concept, Danckwerts and Neubert [7] mention it on their paper regarding the symmetries of genetic code-doublets.

Theorem 1.1.

Let $(G,\bullet)$ be a Klein-4 group with e as identity. Then the cyclic subgroup of $(G,\bullet)$ is only contain identity e and another element such that maximum order of cyclic subgroup of $(G,\bullet)$ is 2.

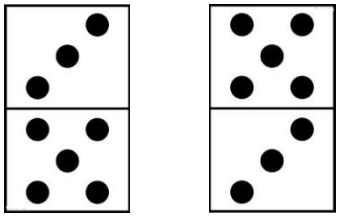
Proof. Let p ∈ G. If $p = e$, then $\{p\}$ is a trivial cyclic subgroup of G. If $p \neq e$, then $p \bullet p = e$. Hence, for any $n, m \in \mathbb{Z}$ we have $p \bullet p = (p^2)^n = e^n = e$. Let m be an odd number. Then we always have n such that $m = 2n + 1$. This fact allowed us to have $p = p^m$, since $p^m = p^{2n+1} = p^{2n} * p = e * p = p$. Therefore, p is the generator of $\{p\}$ and $\{e, p\}$. Then we have prove our assertion.

International Journal of Applied Sciences and Smart Technologies
Volume 2, Issue 1, pages 67–74
p-ISSN 2655-8564, e-ISSN 2685-9432

Domino cards is a set of 28 cards with every card's surface devided in to two boxes and contain the combination of 0 up to 6 dots. We can represent the combination of dots on the card's surfaces as paired of positive integer number as :

(0, 0), (0, 1), (0, 2), (0, 3), (0, 4), (0, 5), (0, 6),
(1, 1), (1, 2), (1, 3), (1, 4), (1, 5), (1, 6),
(2, 2), (2, 3), (2, 4), (2, 5), (2, 6),
(3, 3), (3, 4), (3, 5), (3, 6),
(4, 4), (4, 5), (4, 6),
(5, 5), (5, 6),
(6, 6).

We also need to remind that for domino card, $(p, q) = (q, p)$ where $0 \leq p, q \leq 6$. Hence there are no two or more than two cards in a set of domino cards consists the same number of dots on their surfces. We can look for this example in Figure 1 below :



(3, 5) (5, 3)

Figure 1. Domino card

Further, in the next section we will discuss about the principle of Klein-4 groups which applied to domino cards as our main discuss section.

2 Klein-4 Group Principle On Domino Card

Suppose we have a Klein-4 group $(G, \bullet)$ with elements are four different domino cards. Let us define the binary operation $\bullet$: *deleting the same pattern on card*. This binary operation will implies $\bullet$ only be able to operate between two cards which have at least one side the same pattern. For example

(6, 1) • (0, 6) = (0, 1)
(3, 0) • (0, 2) = (2, 3)
(6, 6) • (6, 6) = (0, 0)

Volume 2, Issue 1, pages 67–74
p-ISSN 2655-8564, e-ISSN 2685-9432

Following Klein-4 group definition, we need to have four different cards as elements including the identity.

Theorem 2.1.
Let $(G,\bullet)$ be a Klein-4 group with $\bullet$ define as "deleting the same pattern on card". Then $(0,0)$ is the identity.
Proof. Let (p,q) be an arbitrary card element of $(G,\bullet)$ such that $0 \leq p,q \leq 6$. Since we need to have a card which operated by $\bullet$ to it self produces identity, then $(p,q) \bullet (p,q)$ will implies p deleting p and q deleting q, hence we have $(p,q) \bullet (p,q) = (0,0)$. Then we obtain our assertion.

Remark 2.2.
Remaining three elements of Klein-4 group are defined as the combination of $(p,q) \bullet (q,r) = (p,r)$, where $0 \leq p,q,r \leq 6$.

As we stated $(0,0)$ to be our identity, here we attach all combinations of possible elements of Klein-4 group on Domino card with binary operation $\bullet$. We can see all the combination in Table 2 below :

Table 2. Combinations of all possible elements

e	a	b	c
(0,0)	(0,1)	(1, 2) (1, 3) (1, 4) (1, 5) (1, 6)	(0, 2) (0, 3) (0, 4) (0, 5) (0, 6)
	(0,2)	(2, 3) (2, 4) (2, 5) (2, 6)	(0, 3) (0, 4) (0, 5) (0, 6)
	(0,3)	(3, 4) (3, 5) (3, 6)	(0, 4) (0, 5) (0, 6)
	(0,4)	(4, 5) (4, 6)	(0, 5) (0, 6)
	(0,5)	(5, 6)	(0, 6)

Volume 2, Issue 1, pages 67–74
p-ISSN 2655-8564, e-ISSN 2685-9432

Theorem 2.3.
Let (p, q) be a non-identity element of $(G,\bullet)$. Maximum order of (p, q) is 2.
Proof. Since (p, q) is a non-identity of $(G,\bullet)$, then value of both of p and q are between 0 and 6 where $p = 0$ and $q = 0$ will not exists on the same card. This condition leads us to $(p, q)^1 = (p, q)$ and $(p, q)^2 = (p, q) \bullet (p, q) = e$. Then we obtain our assertion.

3 Conclusion

Klein 4 group is a simple group consists of four elements including one of them as identity. Many researchers found its application in real life over many field outside of mathematics. This paper presented one more its application by using domino cards as elements by choosing one well define binary operation and many important supporting theorem. Finally the porpose of this paper has been achieved.

References

[1] M. Eie and S. T. Chang, *A Course on Abstract Algebra*, World Scientific, Singapore, 2009.

[2] W. K. Nicholson, *Introduction to Abstract Algebra Fourth Edition*. Wiley, USA, 2012.

[3] J. A. Gallian, *Contemporary Abstract Algebra Eighth Edition*, BROOKS/COLE CEN- GAGE Learning, USA, 2016.

[4] J. Minac and S. Chebolu, "Representations of the miraculous klein group", *Ramanujan Mathematics Society Newsletter*, **22** (1), $135 - 145$, 2012.

[5] S. H. Tsok and I. B. Mshelia, "Application of Group Theory to a Local Game Called "*Tsorry Checkerboard*" (A Case of Klein Four- Group)", *IOSR Journal of Mathematics*, **7** (3), $4 - 6$, 2013.

Volume 2, Issue 1, pages 67–74

p-ISSN 2655-8564, e-ISSN 2685-9432

[6] E. A. Rietman, R. L. Karp and J. A. Tuszynski, " Review and application of group theory to molecular systems biology ", *Theoretical Biology and Medichal Modeling,* **8** (21),$1-29$, (2011).

[7] H. J. Danckwerts and D. Neubert, "Symmetries of genetic code-doublets", *Journal of Molecular Evolution* **5**, $327-332$,(1975).

International Journal of Applied Sciences and Smart Technologies

Volume 2, Issue 1, pages 67–74

p-ISSN 2655-8564, e-ISSN 2685-9432

This page intentionally left blank

International Journal of Applied Sciences and Smart Technologies

Volume 2, Issue 1, pages 75–88

p-ISSN 2655-8564, e-ISSN 2685-9432

Smart Campus Mobile Application Toward the Development of Smart Cities

Tanweer Alam[1,*], Yazeed Mohammed Alharbi[1], Firas Adel Abusallama[1], Ahmad Osama Hakeem[1]

[1]*Department of Computer Science, Faculty of Computer and Information Systems, Islamic University of Madinah, Saudi Arabia*

[*]*Corresponding Author: tanweer03@iu.edu.sa*

(Received 23-01-2020; Revised 09-02-2020; Accepted 09-02-2020)

Abstract

Smart Campus is an android mobile application that has strong features to facilitates students, faculties, admins, parents, and managers. It provides a comprehensive integrated solution to improve the overall performance of the college. The use of mobile applications is increasing day by day. We all use the mobile application in a lot of things in our daily life. We came up with an idea of building an application that will help the students and faculty member to accesses the system as fast as possible. In this study, we will discuss the problem and propose a solution to it, as we will talk about the planning phase and its component, requirements the functional and non-functional with its Data Flow Diagram, etc. We also design the interfaces. This mobile application will help the students and faculty members to do the tasks in the minimum time.

Keywords: mobile application, android, smart campus, smart cities.

International Journal of Applied Sciences and Smart Technologies
Volume 2, Issue 1, pages 75–88
p-ISSN 2655-8564, e-ISSN 2685-9432

1 Introduction

The problem in this situation is about time if you want to check in the system you have to go to the browser, next search about the university, then looking for the page to help for go on the system put if we have an application we will shortcut a lot of steps to go on it. After we studied the problem and knowing the student's and faculty member's needs [1]. We decided to create a mobile application that will serve those who need to do his tasks such as check the schedule, add and remove a course, and many other functions [18,19]. Develop a software platform to be able to access the digital college system as fast as possible.

a. Collect requirements about students and faculty members.
b. Analyze the collected requirements and propose solutions to these problems.
c. Attract the largest number of students and faculty members.
d. Students and faculty members can use the system at any time and easy to use.

What makes our application different than the other applications we talked about (Islamic university)? After we installed the application and tested, we explored that application depends on the web page for the Islamic university, it created as an interface [4, 5, 6]. Actually, all icons linked by the web pages there is no database depend on it. For example, if a student wants to show the schedule, he will click on the icon on the academic system then will transfer to the web page for Islamic university [7,8,9,10]. Also, the problem with this system is that it is supported only by the Arabic language. That application creates just for the students it does not support faculty members and deans [11,12,13,14]. However, in our application, there is a database. It is an independent application that does not depend on web pages. Also, it supports English language. It can use by students, faculty members, and deans.

The rest of the paper is organized as follows. The related works are explained in section 2, the research methodologies are explained in section 3, results and discussion are explained in section 4, and the conclusion is explained in section 5.

International Journal of Applied Sciences and Smart Technologies
Volume 2, Issue 1, pages 75–88
p-ISSN 2655-8564, e-ISSN 2685-9432

2 Related works

This article is based on ideas from several experts, including :

1. Imam Muhammad bin Saud University

The official application of the Imam Mohammed bin Saud Islamic University provides application services for many of the employees of the university students, staff, faculty members, visitors, and others [15, 16, 17]. The application provides the most important news and announcements and events about the university in addition to university maps and academic calendar and telephone directory and others [2]. The most important services of students: student information, schedule, grades, exam schedule, etc. The most important services of staff and faculty: salaries - vacations - allowances - inboxes. There are obtains as shown in Figure 1.



Figure 1. Imam Muhammad bin Saud University

2. Qassim University Application

Qaseem University online service in Figure 2 is a mobile application that aim is to provide communication with students, faculties, management etc. Also, students can add, remove courses for their schedule, show marks, transcripts, and plan [3, 19].

International Journal of Applied Sciences and Smart Technologies

Volume 2, Issue 1, pages 75–88

p-ISSN 2655-8564, e-ISSN 2685-9432

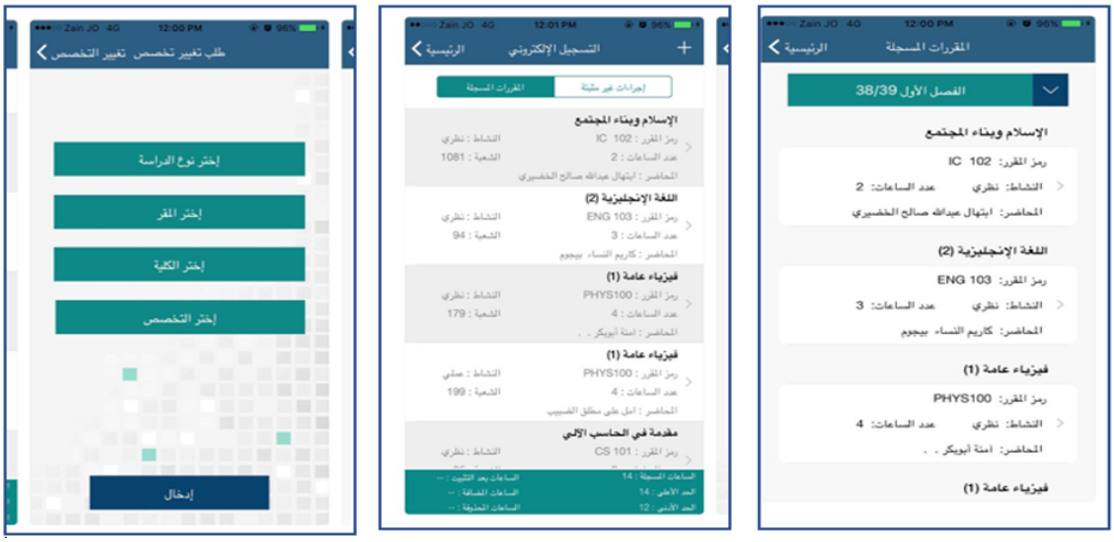


Figure 2. Qassim University application

3. Islamic University Mobile Application:

   You can follow through the application in Figure 3 :

   a. University news and announcements
   b. Access to the university's personal account
   c. Booking travel administration dates
   d. View the names of the admissions
   e. University calendar
   f. Follow the requests of the university administration and communicate with the Rector.
   g. Save your notes in the application (days and tests)
   h. Department of Messages Received

International Journal of Applied Sciences and Smart Technologies

Volume 2, Issue 1, pages 75–88

p-ISSN 2655-8564, e-ISSN 2685-9432

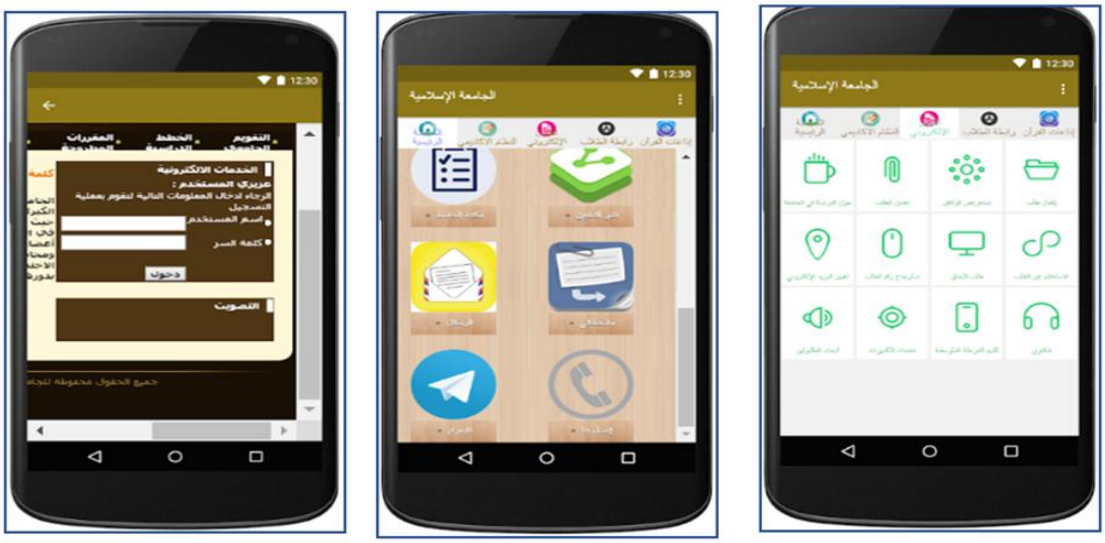


Figure 3. Islamic University.

3 Research Methodology

This diagram explains how the user can enter the system we mean by user (Student, Faculty Member, Manager, Admin) when the user opens the application he will enter his user name and password then the application will check with database, the databases response message [20, 21] to the application if the user name and password match in the database he will enter to home page otherwise reject. There are obtains as shown in Figure 4 below.

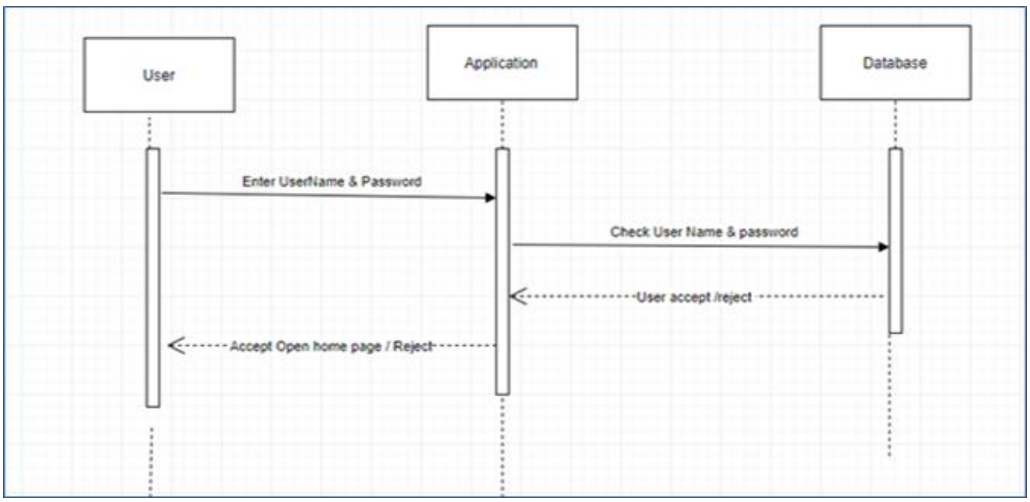


Figure 4. Login to the system

International Journal of Applied Sciences and Smart Technologies
Volume 2, Issue 1, pages 75–88
p-ISSN 2655-8564, e-ISSN 2685-9432

In Figure 5 there is the following sequence diagram, show how the admin give approve to account by choose account in the application then give him approve in the database after that the approved account can enter the system

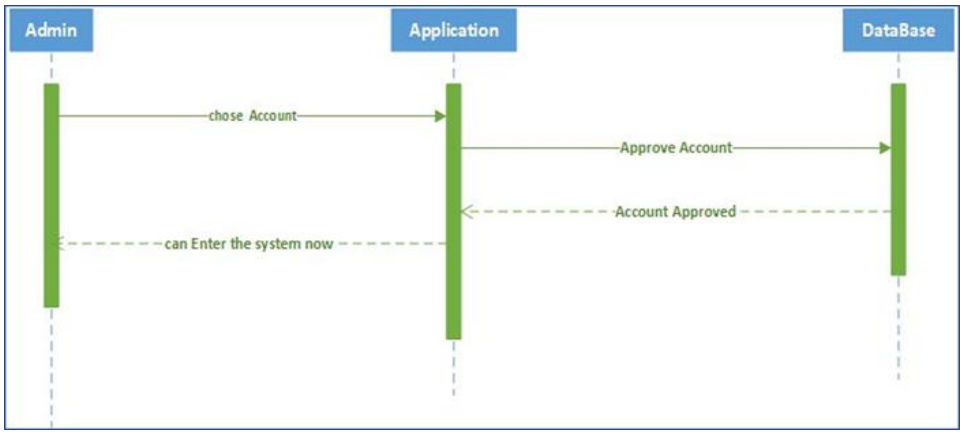


Figure 5. Approve account

The next sequence diagram shows how the student can add or remove a course from his schedule [22, 23]. If the student wants to add a course first choose course name in the application. It will add the course to the database and the database will response message to the application then the course will be in the student schedule.

Remove course is similar to add the course. The student will choose a course in the application, then the course will be deleted from the database. The database will respond message to the application course removed. Course removed from the student schedule. This is obtains as shown in Figure 6.

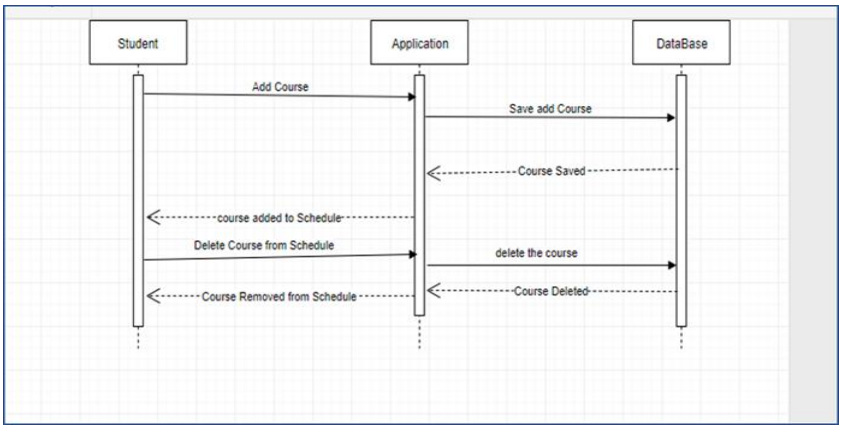


Figure 6. Add/remove course

International Journal of Applied Sciences and Smart Technologies
Volume 2, Issue 1, pages 75–88
p-ISSN 2655-8564, e-ISSN 2685-9432

The following diagram explains how the student can evaluate the courses and faculty members through questionaries. After the student selectsa specific course in the application, he will start the evaluation of the course and faculty member and submit the evaluation to the application [24, 25]. The application in Figure 7 will store the submission in the database. The database will respond message to the application evaluation stored.

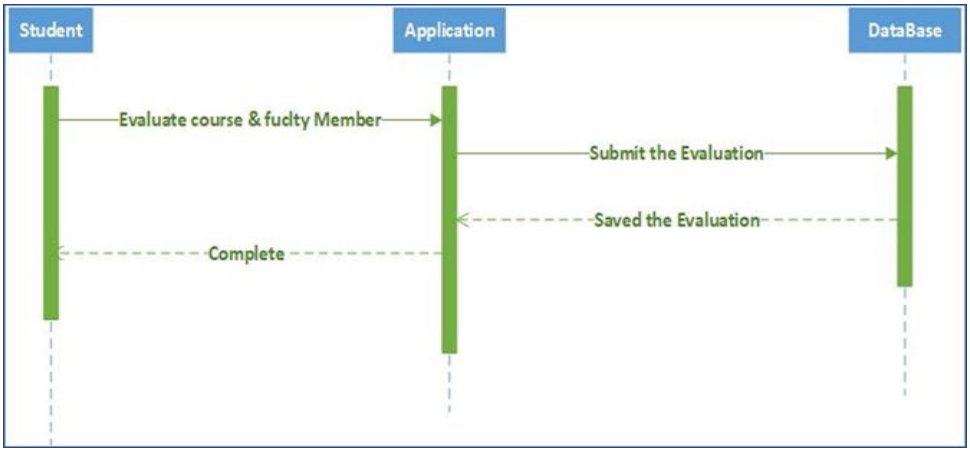


Figure 7. Evaluate course and faculty member

The Following sequence diagram shows how Faculty member set marks for students. After choosingthe student the faculty member can set the marks in the application. The application will store the marks in the database [26, 27, 28]. The database will respondto message marks stored. The application will show the marks in Figure 8.

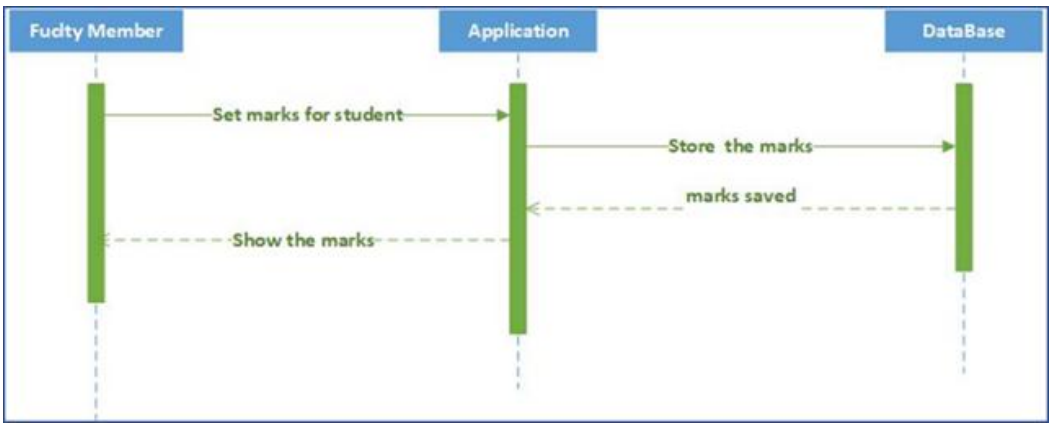


Figure 8. Set marks to student

International Journal of Applied Sciences and Smart Technologies
Volume 2, Issue 1, pages 75–88
p-ISSN 2655-8564, e-ISSN 2685-9432

The next diagram shows how a manager can give permission. After selecting students or faculty members and determine the type of permission in the application. The application will update the database. The database will respondto the message the student or faculty member has permission for the application. Students or faculty members can now use the new permission. That is obtains as shown in Figure 9.

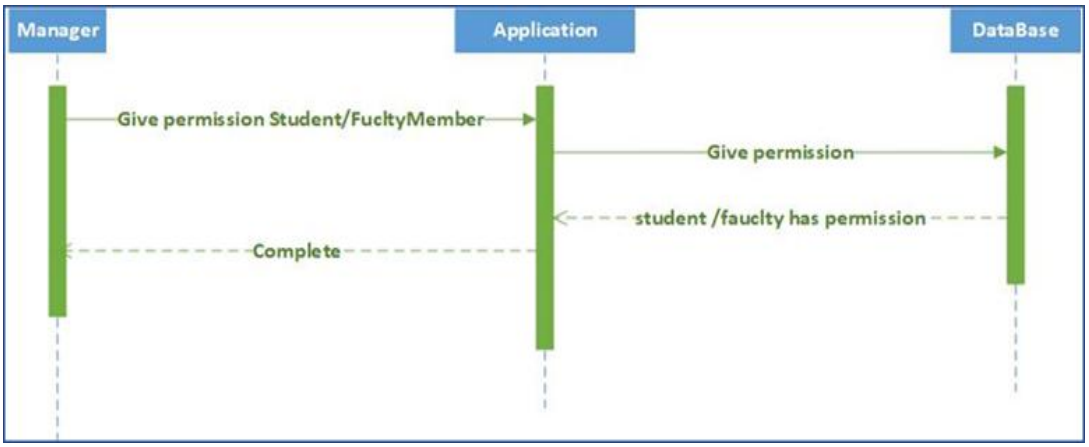


Figure 9. Give permission from the manager

The following sequence diagram in Figure 10 explains how the admin update data. First, the admin will select the user (student, faculty member, manager) and change data in the application [29, 30, 31]. The application will store the data in the database. The database will respond message to the application data updated [32, 33]. The application will show the updated data.

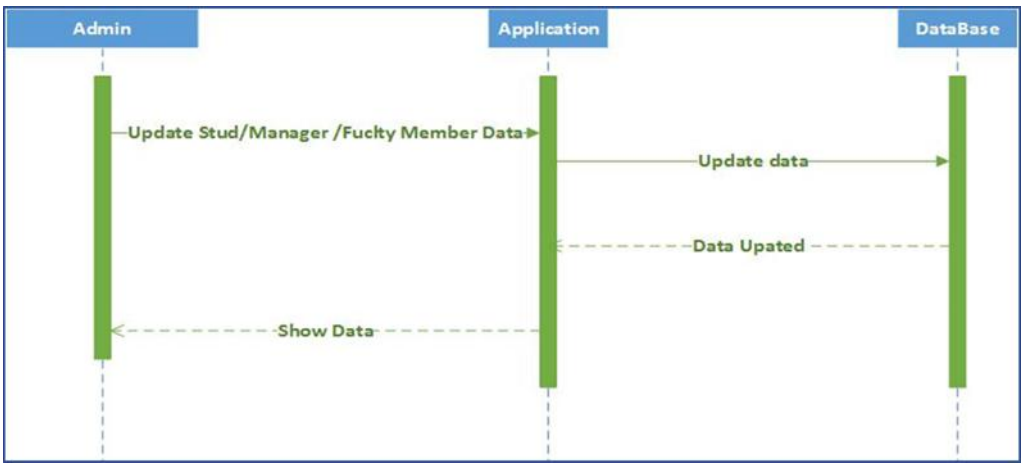


Figure 10. Update data from admin

International Journal of Applied Sciences and Smart Technologies
Volume 2, Issue 1, pages 75–88
p-ISSN 2655-8564, e-ISSN 2685-9432

4 Results and Discussions

The first interface is the login interface.It let the user enter his name and his password to enter into the application. There is a forget password button for the turn to another page to create a new password. In addition, the sing up button for a turn to the page to create new accounts. There are obtains as shown in Figure 11, 12, and 13 below:

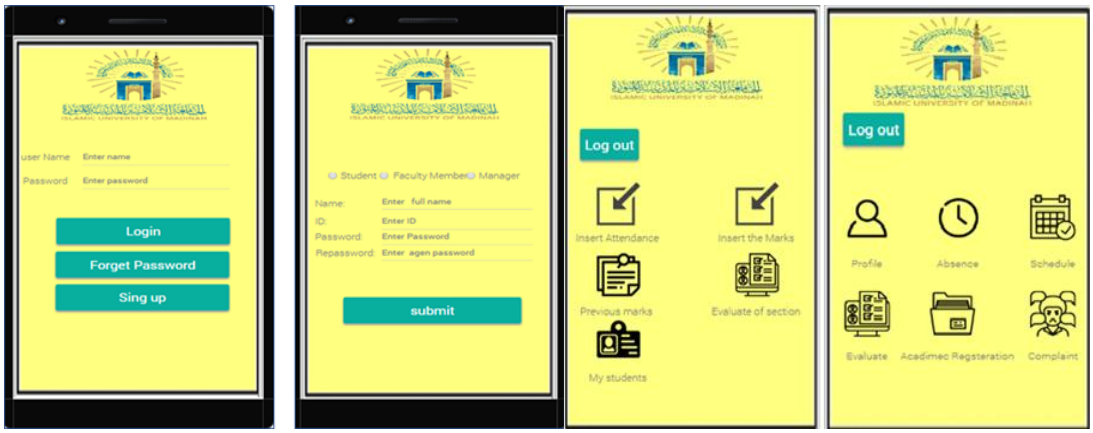


Figure 11. Application interfaces

This is the registry interface and you have the option of choosing between student, faculty, and administrator. To complete registration in the application. Username, password, and repeat password are necessary. This is the main menu interface for a student. There are processes for students such as showing profiles, absence, schedule, and academic registration. Also can do evaluate for the courses. This is the main menu interface for faculty members. There are processes for faculty members such as showing the evaluation of section and previous marks. In addition, they can make some operations such as insert attendance and marks.This is the registry interface and you have the option of choosing between student, faculty, and administrator. To complete registration in the application. Username, password, and repeat password are necessary. This is the main menu interface for a student. There are processes for students such as showing profiles, absence, schedule, and academic registration. Also can do evaluate for the courses. This is the main menu interface for faculty members. There are processes

Volume 2, Issue 1, pages 75–88

p-ISSN 2655-8564, e-ISSN 2685-9432

for faculty members such as showing the evaluation of section and previous marks. In addition, they can make some operations such as insert attendance and marks.



Figure 12.Application interfaces



Figure 13.Application interfaces

5 Conclusions

The authors have done all the initiation processes that start from problem statement moving through the proposed solution into objectives and the aim. We studied and clarify three of related work that has some similarity of our project, which are 'application of the Imam Mohammed bin Saud University, Qassim University

Volume 2, Issue 1, pages 75–88

p-ISSN 2655-8564, e-ISSN 2685-9432

Application, Islamic University Application. Each one of them has one or more properties we are going to use in our application, also they have some negative we must avoid. The survey is done for information gathering from users. We collected the information that we gathered from the survey and we analyzed it, some UML Diagrams and Data Flow Diagrams as well as, the interface at the end. We have worked hard and diligent in this project, and believe we have done very well, and hope that everyone likes and uses our application, and making their life easier, and that's what we've tried to achieve for them.

References

[1] *A Comprehensive Education Management Suite*, http://www.auromeera.com/ (Accessed on 10-02-2020).

[2] Al Imam University, https://play.google.com/store/apps/details?id=com.imamuniversity.app&hl=ar (Accessed on 10-02-2020).

[3] Al Qaseem University, http://cutt.us/uKdaZ (Accessed on 10-02-2020).

[4] A. Tanweer, "5G-Enabled Tactile Internet for smart cities: vision, recent developments, and challenges", *Jurnal Informatika*, **13** (2), 1 – 10, 2019.

[5] V. R. Ganesh, "Android College Management System", *International Journal of Advanced Research in Computer Engineering & Technology*, **5** (4) 882 – 885, 2016.

[6] N. M. Z. Hashim and S. N. K. S. Mohamed, "Development of Student Information System", *International Journal of Science and Research (IJSR)*, **2** (8), 256 – 260, 2013.

[7] *What is SDLC Waterfall Model ?*, http://cutt.us/tHhIF (Accessed on 10-02-2020).

[8] M. Rouse, *Requirements analysis*, 2007, http://cutt.us/3di7W (Accessed on 10-02-2020).

[9] U. Eriksson, *The difference between functional and non-functional requirements*. 2015, http://cutt.us/5ICJ1 (Accessed on 10-02-2020).

[10] Bisk. *What is SWOT Analysis?* http://cutt.us/XmfjA. (Accessed on 10-02-2020).

[11] *Use case diagram*, http://cutt.us/sQ4Me (Accessed on 10-02-2020).

Volume 2, Issue 1, pages 75–88

p-ISSN 2655-8564, e-ISSN 2685-9432

[12] Islamic university, http://cutt.us/oqDrP (Accessed on 10-02-2020).

[13] *Just In Mind*, http://cutt.us/1RnZI (Accessed on 10-02-2020).

[14] *Sequence Diagram*, http://cutt.us/S38IQ (Accessed on 10-02-2020).

[15] A. Tanweer and M. Benaida, "The Role of Cloud-MANET Framework in the Internet of Things (IoT)", *International Journal of Online Engineering (iJOE)*, **14** (12), 97−110, 2018.

[16] A. Tanweer, "Middleware Implementation in Cloud-MANET Mobility Model for Internet of Smart Devices", *International Journal of Computer Science and Network Security*, **17** (5), 86 −94, 2017.

[17] A. Tanweer and M. Benaida, "CICS: Cloud–Internet Communication Security Framework for the Internet of Smart Devices", *International Journal of Interactive Mobile Technologies (IJIM*). **12** (6), 74−84, 2018

[18] A.Tanweer and B. Rababah, "Convergence of MANET in Communication among Smart Devices in IoT", *International Journal of Wireless and Microwave Technologies(IJWMT)*, **9** (2), 1−10, 2019.

[19] A. Tanweer, "IoT-Fog: A Communication Framework using Blockchain in the Internet of Things", *International Journal of Recent Technology and Engineering (IJRTE)*, **7** (6), 2019.

[20] A. Tanweer, "Blockchain and its Role in the Internet of Things (IoT)", *International Journal of Scientific Research in Computer Science, Engineering and Information Technology*, **5** (1), 151−157, 2019.

[21] A. Tanweer, "A reliable framework for communication in internet of smart devices using IEEE 802.15.4", *ARPN Journal of Engineering and Applied Sciences*, **13** (10), 3378−3387, 2018.

[22] A. Tanweer, "A Reliable Communication Framework and Its Use in Internet of Things (IoT)", *International Journal of Scientific Research in Computer Science, Engineering and Information Technology (IJSRCSEIT)*, **3** (5), 450−456, 2018.

[23] A. Tanweer and M. Aljohani, "Design and implementation of an Ad Hoc Network among Android smart devices", *Green Computing and Internet of Things (ICGCIoT)*, 1322−1327, 2015.

[24] A. Tanweer and M. Aljohani, "An approach to secure communication in mobile ad-hoc networks of Android devices", *International Conference on Intelligent Informatics and Biomedical Sciences (ICIIBMS)*, 371−375, 2015.

[25] M. Aljohani and A. Tanweer, "An algorithm for accessing traffic database using wireless technologies", *Computational Intelligence and Computing Research (ICCIC), IEEE International Conference*, 1−4, 2015.

[26] A. Tanweer and M. Aljohani, "Design a new middleware for communication in ad hoc network of android smart devices", *Proceedings of the Second International Conference on Information and Communication Technology for Competitive Strategies*, 1−6, 2016.

[27] A. Tanweer, "Fuzzy control based mobility framework for evaluating mobility models in MANET of smart devices", *ARPN Journal of Engineering and Applied Sciences*, **12** (15) , 4526−4538, 2017.

[28] A. Tanweer, A. P. Srivastava, S.Gupta and R. G. Tiwari, "Scanning the Node Using Modified Column Mobility Model", *Computer Vision and Information Technology: Advances and Applications*, 455, 2010.

[29] A. Tanweer and B. K. Sharma, "A New Optimistic Mobility Model for Mobile Ad Hoc Networks", *International Journal of Computer Applications*, **8** (3), 1−4 , 2010.

[30] A. Tanweer, "Cloud Computing and its role in the Information Technology", *IAIC Transactions on Sustainable Digital Innovation (ITSDI)*, **1** (2), 108 − 115. 2020.

[31] A. Tanweer, A. S. Salem, A. O. Alsharif, and A. M. Alhejaili, "Smart Home Automation Towards the Development of Smart Cities", *APTIKOM Journal on Computer Science and Information Technologies*, **5** (1).2020.

[32] M. Aljohani and A. Tanweer, "Design an M-learning framework for smart learning in ad hoc network of Android devices," *Proceedings of Computational Intelligence and Computing Research, IEEE International Conference on*, 1 − 5, 2015.

Volume 2, Issue 1, pages 75–88

p-ISSN 2655-8564, e-ISSN 2685-9432

[33] M. Aljohani and A. Tanweer. "Real Time Face Detection in Ad Hoc Network of Android Smart Devices", *Advances in Computational Intelligence : Proceedings of International Conference on Computational Intelligence.*245 – 255 2015.

International Journal of Applied Sciences and Smart Technologies

Volume 2, Issue 1, page 89

p-ISSN 2655-8564, e-ISSN 2685-9432

AUTHOR GUIDELINES

Author guidelines are available at the journal website:
http://e-journal.usd.ac.id/index.php/IJASST/about/submissions#authorGuidelines